Excited States of the Mirror Nuclei, Li^7 and Be^7

A. B. BROWN, C. W. SNYDER, W. A. FOWLER, AND C. C. LAURITSEN
*Kellogg Radiation Laboratory, California Institute of Technology, Pasadena, California**
(Received December 28, 1950)

By studying the alpha-particles emitted in the disintegration of B^{10} by protons it has been shown that there exists an excited state in Be^7 at 434.4±4 kev which corresponds to the well-known first excited state in the mirror nucleus, Li^7. Measurements on the inelastic scattering of protons in Li^7 yield a value 479.0±1.0 kev for the energy of the Li^{7*}. The existence of these mirror states adds support to the equality of the *p-p* and *n-n* interactions exclusive of electrostatic and magnetic forces. The small difference, 45±4 kev, in the excitation energies is larger than second-order electric effects and is believed to be consistent with the order of magnitude of magnetic interactions in nuclei. The splitting of the ground and excited states must arise in some specific property of the nuclear interactions. In connection with the energy determinations, a detailed discussion is given of the precise measurements of the *Q*-values of nuclear reactions employing high resolution analyzers, electrostatic and magnetic, in the determination of particle energies. Experimental determinations of the cross sections for $B^{10}(p,\alpha)Be^7$, $B^{10}(p,\alpha')Be^{7*}(\gamma)Be^7$, $B^{10}(p,p)B^{10}$, $Li^7(p,p)Li^7$, and $Li^7(p,p')Li^{7*}(\gamma)Li^7$ are given.

I. INTRODUCTION

EARLY investigations[1] in this laboratory of the maximum kinetic energy of the positrons emitted by the light radioactive nuclei $_6C^{11}$, $_7N^{13}$, and $_8O^{15}$ showed that these nuclei differed in mass from their mirror isobars $_5B^{11}$, $_6C^{13}$, and $_7N^{15}$, respectively, by amounts which are quite simply calculable from the electrostatic energies[1a] of the nuclei and the small difference in the masses of neutron and proton. This indicated that the intrinsic nuclear interactions among any group of nucleons is unchanged if the neutrons are replaced by protons and vice versa. On the assumption of two body forces, this indicated further that the force between pairs of neutrons is equal to that between pairs of protons except for the repulsive electrostatic interaction. This equality had been suggested by the approximately linear variation of the binding energy of nuclei with atomic weight[2] and explained, in a very straightforward way, the fact that the stable nuclei consist of approximately equal numbers of neutrons and protons, the small excess of neutrons being directly attributable to the repulsive electrostatic forces between protons.

In subsequent investigations[3] it was found that the same conclusions could be drawn from measurements on the positron energy of all the radioactive transitions involving the mirror nuclei with $A=2Z+1$ up to $A=41$. For $Sc^{41}(\beta^+)Ca^{41}$ the maximum positron energy of 4.94 Mev can be accurately calculated even though the total nuclear binding is of the order of 400 Mev for $A=41$, showing that the nuclear binding must be the same for Sc^{41} and Ca^{41} within very narrow limits. Additional strong evidence is afforded by the difference in mass of Be^7 and Li^7 and of H^3 and He^3 in which cases the electrostatic effects are small and *K*-capture and electron emission, rather than positron emission, occur. Recent experimental determinations[4] of the mass differences of the radioactive mirror nuclei for which $A=2Z\pm2$ can be summarized as follows: $_5B^8-{}_3Li^8=2.0$ Mev, $_6C^{10}-{}_4Be^{10}=3.5$ Mev, $_7N^{12}-{}_5B^{12}=4.2$ Mev, $_8O^{14}-{}_6C^{14}=4.9$ Mev, $_{11}Na^{20}-{}_9F^{20}=8.3$ Mev. These are consistent with the conclusions discussed above, but the mass-energy differences have not been as precisely determined as those for $A=2Z\pm1$.

The electrostatic energy of a nucleus arising from the mutual repulsion of the protons in the nucleus can be expressed[1] as

$$U_E=\tfrac{1}{2}Z(Z-1)e^2\langle 1/r\rangle, \quad (1)$$

where $\langle 1/r\rangle$ is the average of the reciprocal of the distance between all possible pairs of protons in the nucleus. It is usually assumed that the effect of the relatively weak electrostatic forces can be calculated by perturbation methods using the proton distribution determined by the nuclear forces only and that the electrostatic energy can be superimposed on the intrinsic nuclear energy without higher order corrections. On the additional assumption of constant nuclear density out to a radius $R=R_0A^{\frac{1}{3}}$, which is indicated by numerous other nuclear phenomena, one can also write

$$U_E=3Z(Z-1)e^2/5R=3Z(Z-1)e^2/5A^{\frac{1}{3}}R_0. \quad (1')$$

The difference in electrostatic energy for mirror nuclei for which $A=2Z\pm n$ is then given by[4a]

$$\delta U_E=\tfrac{1}{2}n(A-1)e^2\langle 1/r\rangle=3n(A-1)e^2/5A^{\frac{1}{3}}R_0. \quad (2)$$

* This work was assisted by the joint program of ONR and AEC.

[1] Fowler, Delsasso, and Lauritsen, Phys. Rev. **49**, 561 (1936).

[1a] It was assumed that magnetic terms were small.

[2] L. A. Young, Phys. Rev. **47**, 972 (1935); **48**, 913 (1935).

[3] White, Delsasso, Fox, and Creutz, Phys. Rev. **56**, 512 (1939). White, Creutz, Delsasso, and Wilson, Phys. Rev. **59**, 63 (1941). L. D. P. King and D. R. Elliott, Phys. Rev. **58**, 846 (1940); **59**, 403 (1941).

[4] Sherr, Muether, and White, Phys. Rev. **75**, 282 (1949). L. Alvarez, University of California Radiation Lab. Report 739, May 31 (1950); Phys. Rev. **75**, 1815 (1949).

[4a] We include only the term in δU_E arising from $\delta Z=n$ and neglect any contribution from a difference in $\langle 1/r\rangle$ for the two nuclei. Such contributions will be small and require, in calculation, detailed attention to symmetry properties and higher order effects of the coulomb perturbation.

All of the results discussed in the preceding paragraphs are consistent with the values $e^2/R_0 \approx 2m_0c^2$ or $R_0 \approx 1.4 \times 10^{-13}$ cm. Detailed theoretical calculations have been given by numerous authors.[5]

It has been emphasized by Inglis[6] that because of the Larmor and Thomas precessions there will be a small magnetic contribution to the energy of a nucleus. For an unpaired proton or neutron with orbital angular momentum $l\hbar$ and spin $s\hbar=\frac{1}{2}\hbar$, a very elementary calculation shows that this energy is linear in the nuclear density, $\rho=(4\pi R_0^3/3)^{-1}$, and is given by

$$U_M \sim -(g'e^2\hbar^2/4R_0^3M_p^2c^2)(\mathbf{l}\cdot\mathbf{s}) \sim -5g'(\mathbf{l}\cdot\mathbf{s}) \text{ kev}, \quad (3)$$

where $g'=g_p-1=4.587$ for a proton and $g'=g_n=-3.827$ for a neutron. This expression yields, as an example, a contribution in the separation of ${}_3Li^{7*}-{}_3Li^7$, on the assumption that they are ${}^2P$ states, of approximately 30 kev, as was first noted by Inglis. There is some indication that the nuclear density is anomalously low in Li^7 and that the true value for the magnetic splitting may be somewhat smaller. Spin-orbit forces of an intrinsic nuclear nature such as those discussed recently by Case and Pais[7] may account for the much larger observed splitting which is discussed in this paper.

The difference in magnetic energy for mirror nuclei with $A=2Z\pm1$ is given by

$$\delta U_M \sim \pm\tfrac{1}{4}(g_p-g_n-1)\left(\frac{e^2\hbar^2}{R_0^3M_p^2c^2}\right)\mathbf{l}\cdot\mathbf{s} \sim \pm 50\mathbf{l}\cdot\mathbf{s} \text{ kev}, \quad (4)$$

the plus sign holding for an unpaired proton in the nucleus with $A=2Z+1$ and the minus sign for an unpaired neutron in this nucleus. The magnetic interactions are treated in considerably more detail in the paper by Inglis which follows this one.[7a] The total interaction energy difference for corresponding low lying states of mirror nuclei will be given by $\delta U=\delta U_E+\delta U_M$. Additional complications in states of high excitation are discussed briefly in Sec. VII.

In addition to the equality of neutron-neutron and proton-proton forces, it has been known for some time, from scattering experiments, that the singlet s-wave interaction between neutron and proton was approximately equal to that between pairs of protons if ranges and shapes are assumed to be identical.[8] There exists, however, a small difference, the neutron-proton potential depth exceeding that of two protons by several percent.[9] It has been shown recently[10] that the magnetic interaction between nucleons accounts adequately for this difference if the nuclear potential resembles that of Yukawa. It has also been shown that the anomalous scattering results at very high energies,[11] which seemed to demand inequality in the p-p and singlet n-p forces, can be explained by the introduction of a spin-orbit velocity dependent interaction[7] or by a very short range repulsive interaction between nucleons.[12] There would thus seem to be, at the present time, no conclusive evidence against the hypothesis that nuclear forces are fundamentally charge independent. Complications arising from the exclusion principle, which excludes certain interactions for like particles, must, of course, always be taken into account.

From the charge independence of nuclear forces, and in particular from the equality of neutron-neutron and proton-proton forces it follows that mirror nuclei should have corresponding series of excited quantum states as long as electromagnetic perturbations are not too large. Not only should the difference in energy of the ground states of mirror nuclei be given by a simple electrostatic and magnetic calculation but so also should the differences in energy of the low-lying excited states of these nuclei, with proper allowance being made for the fact that the excited states might have different radii than do the ground states and also different spin-orbit values and orientations. With the publication in 1948 of a summary of the energy levels of light nuclei,[13] it became clear that very little information was available on the excited states of mirror nuclei. In general, one or both of the pairs fell in the class of nuclei whose energy levels had not been investigated experimentally for one or more of the large variety of reasons which were emphasized in a discussion[14] of the methods of investigating the excited states of light nuclei. It was realized that a definite solution of the problem would await a complete investigation of the level structure of a number of mirror pairs, but it was decided that a start could best be made by a search for an unknown level in one member of a pair corresponding to a well-known level in the other member of the pair.

The most carefully and completely investigated excited state in light nuclei is the excited state of Li^7 at 479 kev. This is illustrated in Table I where we list the numerous measurements which have been made on the energy of this state. We give, in the table, a complete list of references on determinations of the energy of this state, some of which will be discussed further in the following. The existence of this state was first indicated by the detection of gamma-rays from the non-capture excitation of lithium with alpha-particles

[5] E. Feenberg and E. Wigner, Phys. Rev. **51**, 95 (1937); E. Wigner, Phys. Rev. **51**, 106, 947 (1937), **56**, 519 (1939); H. A. Bethe, Phys. Rev. **54**, 436 (1938); and E. Feenberg and G. Goertzel, Phys. Rev. **70**, 597 (1946).

[6] D. R. Inglis, Phys. Rev. **50**, 783 (1936).

[7] K. M. Case and A. Pais, Phys. Rev. **79**, 185 (1950).

[7a] D. R. Inglis, Phys. Rev. **82**, 181 (1951).

[8] Breit, Condon, and Present, Phys. Rev. **50**, 825 (1936).

[9] Breit, Hoisington, Share, and Thaxton, Phys. Rev. **55**, 1103 (1939).

[10] J. Schwinger, Phys. Rev. **78**, 135 (1950).

[11] R. S. Christian and E. W. Hart, Phys. Rev. **77**, 441 (1950); **79**, 85 (1950).

[12] R. Jastrow, Phys. Rev. **79**, 389 (1950).

[13] W. F. Hornyak and T. Lauritsen, Revs. Modern Phys. **20**, 191 (1948). T. Lauritsen, N.R.C. Preliminary Report No. 5 (1949), and Hornyak, Lauritsen, Morrison, and Fowler, Revs. Modern Phys. **22**, 291 (1950).

[14] Lauritsen, Fowler, and Lauritsen, Nucleonics **2**, No. 4, 18 (1948).

TABLE I. Measurements of the excitation energy of Li^{7*}.

Investigators	Reference	Reaction	Method	Energy (kev)
Bothe and Becker	Z. Physik **66**, 289 (1930).	$Li^7(\alpha,\alpha')Li^{7*}$	detected γ-rays	—
Webster	Proc. Roy. Soc. (London) **136**, 428 (1932).	$Li^7(\alpha,\alpha')Li^{7*}$	γ-absorption	600±100
Savel	Comptes rend. **198**, 1404 (1934).	$Li^7(\alpha,\alpha')Li^{7*}$	γ-absorption	500
Schnetzler	Z. Physik **95**, 302 (1935).	$Li^7(\alpha,\alpha')Li^{7*}$	γ-absorption	500
Delsasso, Fowler and Lauritsen	Phys. Rev. **48**, 848 (1935).	$Li^6(d,p')Li^{7*}$	detected p-groups	—
Bothe	Z. Physik **100**, 273 (1936).	$Li^7(\alpha,\alpha')Li^{7*}$	γ-spectrometer	200?, 390, 590
Rumbaugh, Roberts and Hafstad	Phys. Rev. **50**, 681 (1936). Phys. Rev. **54**, 657 (1938).	$Li^6(d,p')Li^{7*}$	p-group ranges	455±15
Speh	Phys. Rev. **50**, 689 (1936).	$Li^7(\alpha,\alpha')Li^{7*}$	γ-absorption	700±70
Haxel	Z. Physik **104**, 540 (1937).	$B^{10}(n,\alpha')Li^{7*}$	α-group ranges	900
Williams, Shepherd, and Haxby	Phys. Rev. **52**, 390 (1937).	$Li^6(d,p')Li^{7*}$	γ-absorption	400±25
Livingston and Hoffman	Phys. Rev. **53**, 227 (1938).	$B^{10}(n,\alpha')Li^{7*}$	α-group ranges	480
Maier-Leibnitz	Naturwiss. **26**, 614 (1938). Z. Physik **112**, 569 (1939).	$Be^7(K)Li^{7*}$	γ-cloud chamber	425±20
Roberts, Heydenburg, and Locher	Phys. Rev. **53**, 1016 (1938).	$Be^7(K)Li^{7*}$	γ-absorption	425±25
Bower, Bretscher and Gilbert	Proc. Cambridge Phil. Soc. **34**, 290 (1938).	$B^{10}(n,\alpha')Li^{7*}$	α-group ranges	500
O'Ceallaigh and Davies	Proc. Roy. Soc. (London) **167**, 81 (1938).	$B^{10}(n,\alpha')Li^{7*}$	α-group ranges	550±150
Mauer and Fisk	Z. Physik **112**, 436 (1939).	$B^{10}(n,\alpha')Li^7$	total ionization	200, 410, 640, 840?
Fowler and Lauritsen	Phys. Rev. **56**, 841 (1939).	$Li^7(p,p')Li^{7*}$	γ-absorption	495±25
Hudson, Herb, and Plain	Phys. Rev. **57**, 587 (1940).	$Li^7(p,p')Li^{7*}$	γ-absorption	459
Graves	Phys. Rev. **57**, 855 (1940).	$Be^9(d,\alpha)Li^{7*}$	α-group ranges	494±16
Wilson	Proc. Roy. Soc. (London) **177**, 382 (1941).	$B^{10}(n,\alpha')Li^{7*}$	total ionization	420±50
Zlotowski and Williams	Phys. Rev. **62**, 29 (1942).	$Be^7(K)Li^{7*}$	γ-coincidence counters	485±5
Bøggild	Kgl. Danske. Videnskab Selskab Math.-fys. Medd. **23**, No. 4 (1945).	$B^{10}(n,\alpha')Li^{7*}$	total range	420
Rubin	Phys. Rev. **69**, 134 (1946).	$Be^7(K)Li^{7*}$	γ-absorption	476±10
Siegbahn and Slätis	Arkiv. f. Ast. Math-Fys. **34A**, No. 15 (1946).	$Li^7(\alpha,\alpha')Li^{7*}$	γ-spectrometer	462
Siegbahn	Arkiv. f. Ast. Math-Fys. **34B**, No. 6 (1946).	$Be^7(K)Li^{7*}$	γ-spectrometer	453±5
Gilbert	Proc. Cambridge Phil. Soc. **44**, 447 (1948).	$B^{10}(n,\alpha')Li^{7*}$	α-Li^7 group ranges	500±40
Zaffarano, Kern and Mitchell	Phys. Rev. **74**, 105 (1948).	$Be^7(K)Li^{7*}$	γ-spectrometer	474±4
Kurie and Ter-Pogossian	Phys. Rev. **74**, 677 (1948).	$Be^7(K)Li^{7*}$	γ-spectrometer	485±5
Buechner, *et al.*	Phys. Rev. **74**, 1569 (1948).	$Be^9(d,\alpha')Li^{7*}$	α-spectrometer	482±3
Buechner, *et al.*	Phys. Rev. **74**, 1569 (1948).	$Li^6(d,p)Li^{7*}$	p-spectrometer	483±6
Elliott and Bell	Phys. Rev. **74**, 1869 (1948).	$B^{10}(n,\alpha')Li^{7*}$	γ-spectrometer	478.5±1.5
Stebler, Huber and Bicksel	Helv. Phys. Acta. **22**, 362 (1949).	$B^{10}(n,\alpha')Li^{7*}$	total ionization	490±20
Rasmussen, Hornyak and Lauritsen	Phys. Rev. **76**, 581 (1949).	$Be^7(K)Li^{7*}$	γ-spectrometer	476.6±0.8
Rasmussen, Hornyak and Lauritsen	Phys. Rev. **76**, 581 (1949).	$Be^9(d,\alpha')Li^{7*}$	γ-spectrometer	472
Hornyak, Lauritsen and Rasmussen	Phys. Rev. **76**, 731 (1949).	$Li^7(p,p')Li^{7*}$	γ-spectrometer	478.3±0.6[a]
Ter-Pogossian, Robinson, and Goddard	Phys. Rev. **76**, 1407 (1949).	$Be^7(K)Li^{7*}$	γ-spectrometer	478.5±0.5
Thomas and Lauritsen	Phys. Rev. **78**, 88 (1950).	$Li^6(d,p')Li^{7*}$	γ-spectrometer	478.5±1[a]
Burcham and Freeman	Phil. Mag. **41**, 337 (1950).	$B^{10}(n,\alpha')Li^{7*}$	α-spectrometer	490±70
This report		$Li^7(p,p')Li^{7*}$	p-spectrometer	479.0±1

[a] No correction for Doppler shifts.

by Bothe and Becker, Webster, Savel, and Schnetzler. The latter two investigators each measured the energy of the gamma-rays as approximately 0.5 Mev and correctly inferred their origin. Two groups of protons were observed in the bombardment of natural lithium targets by Delsasso, Fowler, and Lauritsen. The state was shown to be in the nucleus Li^7 by Rumbaugh and Hafstad, who detected two groups of protons from the reactions $Li^6(d,p)Li^7$ and $Li^6(d,p')Li^{7*}$, using a separated Li^6 target.

Several energy determinations of increased precision were made later, one being made in this laboratory by Rubin, who found an energy of 476±10 Mev by a comparison of the absorption coefficient of the radiation from $Be^7(K)Li^{7*}(\gamma)Li^7$ with that of the annihilation radiation of positrons. In 1949, two methods were used in this laboratory to measure the energy of this state with high precision. A magnetic lens gamma-ray spectrometer was used to measure the energy of the radiation following the inelastic scattering of protons by Li^7. In addition, a double focusing particle spectrometer[15] was employed to measure the difference in energy of the elastically and inelastically scattered protons. A preliminary estimate[16] for the excitation energy was reported. These latter measurements will be discussed in detail as a part of this paper. With these experiments as background, it was considered appropriate to search for a corresponding level in Be^7, the mirror nucleus of Li^7. As Be^7 is not readily available as a target for nuclear disintegration experiments, the most straightforward investigation, namely that of the inelastic scattering of protons by Be^7, was ruled out. It was decided to study the reaction $B^{10}(p,\alpha)Be^7$ and to look for evidence for $B^{10}(p,\alpha')Be^{7*}$. The alpha-particles produced in the bombardment of B^{10} by protons are of

[15] Snyder, Rubin, Fowler, and Lauritsen, Rev. Sci. Inst. **21**, 852 (1950).

[16] Fowler, Lauritsen, and Rubin, Phys. Rev. **75**, 1471 (1949).

TABLE II. Measurements of the excitation energy of Be^{7*}.

Investigators	Reference	Reaction	Method	Energy (kev)
Grosskreutz and Mather	Phys. Rev. **77**, 580, 747 (1950).	$Li^7(p,n)Be^{7*}$	n-groups	205, 470, 745, all ±70
Hall	Phys. Rev. **77**, 411 (1950).	$Li^7(p,n)Be^{7*}$	n-groups	420 to 480
Johnson, Laubenstein and Richards	Phys. Rev. **77**, 413 (1950).	$Li^7(p,n)Be^{7*}$	n-groups	435±15
Whaling and Butler	Phys. Rev. **78**, 72 (1950).	$Li^6(d,n)Be^{7*}$	n-groups	about 400
Hamermesh and Hummel	Phys. Rev. **78**, 73 (1950).	$Li^7(p,n)Be^{7*}$	n-groups	428±20
Lauritsen and Thomas	Phys. Rev. **78**, 88 (1950).	$Li^6(d,n)Be^{7*}$ $B^{10}(p,\alpha)Be^{7*}$	γ, spectrometer	429±5
Gibson and Green	Proc. Phys. Soc. (London) **63**, 494 (1950).	$Li^6(d,n)Be^{7*}$	n-groups	450±60
Burcham and Freeman	Phil. Mag. **41**, 337 (1950).	$B^{10}(p,\alpha)Be^{7*}$	α-groups	about 400
Freier, Rosen, and Stratton	Phys. Rev. **79**, 721 (1950).	$Li^7(p,n)Be^{7*}$	n-groups	428±15
Van Patter, Sperduto, Strait, and Buechner	Phys. Rev. **79**, 900 (1950).	$B^{10}(p,\alpha)Be^{7*}$	α-groups	431±5
Keepin	Phys. Rev. **80**, 768 (1950)	$Li^7(p,n)Be^{7*}$	n-groups	433±26
This report		$B^{10}(p,\alpha)Be^{7*}$	α-groups	434.4±4

low energy and could be analyzed easily in the double focusing magnetic spectrometer mentioned above, with which observations on alpha-particles up to 2 Mev in energy can be made. Furthermore, these reactions are of considerable interest because of their correspondence with the well-known neutron reactions, $B^{10}(n,\alpha)Li^7$ and $B^{10}(n,\alpha')Li^{7*}$. Preliminary results[17] of the investigation of these proton reactions have been presented. Similar results have been obtained at the Massachusetts Institute of Technology.[18] Numerous investigators (Table II) have shown that the excited state occurs in the reaction $Li^6(d,n')Be^{7*}$, and Grosskreutz and Mather have reported evidence for the occurrence of two additional low energy excited states of Be^7 in this reaction. In this laboratory, a careful comparison[19] has been made of the energy of the gamma-rays from the two excited mirror states produced in the mirror reactions $Li^6(d,p')Li^{7*}$ and $Li^6(d,n')Be^{7*}$. These results will be reported in detail separately.

II. THE EXPERIMENTAL ARRANGEMENT

The apparatus used in these experiments has been described previously in detail. The protons for the bombardment were accelerated in the 1.7-Mev electrostatic accelerator[20] of the Kellogg Radiation Laboratory. The energy of these incident protons was determined accurately by passing the beam through a 90°, one meter radius, electrostatic analyzer[21] whose energy resolution is 2×10^{-4} of the bombarding energy. This resolution has been recently ascertained by measurements on the narrow resonance in $Al(p,\gamma)$ at 993 kev. The electrostatic analyzer was calibrated against the resonance at 873.5 kev in the gamma-ray yield from the proton bombardment of fluorine. In making the calibration, corrections were made for relativistic mass changes, for the positive guard potential on the target which was used to avoid the effects of secondary electron emission, for the change of the target potential during bombardment, and for the presence of contamination layers of carbon and oxygen on the target. This last effect was minimized by the use of an auxiliary pumping system and liquid air trap on the target chamber. It is believed that the energy of the protons actually incident on the relevant target material was known to about 0.1 percent on an absolute scale, and for comparison experiments it could be held to 0.02 percent.

The energy of the scattered particles and of the reaction products was measured by a 180°, 26.7-cm radius, double focusing magnetic spectrometer.[15] The spectrometer was calibrated by using protons of known energy leaving the electrostatic analyzer scattered at a known angle into the spectrometer by copper or gold targets. Details of the calibrations are given in the reference cited. The method of determination of the angle of observation of the spectrometer is also discussed in this reference. It is believed that the energy of the products of a reaction could be determined to ±0.1 percent and that the angle was known to ±0.3°. The particles were detected after leaving the magnetic spectrometer by either an ionization chamber or by a scintillation counter.[22] The scintillation counter was found to be especially convenient because it was not necessary to use thin vacuum tight foils before it, as was the case with the ionization chamber.

In those cases in which protons and alpha-particles of the same energy passed through the spectrometer, at a given field setting, into the detector, it was necessary to use auxiliary absorption techniques to distinguish them. Aluminum foils thick enough to stop the alpha-particles but thin enough to pass the protons could be interposed between the spectrometer and the counter, and readings were taken with and without the foils in place. The first reading gave the number of protons, with some small correction for scattering and straggling in the foil, while the difference gave the number of alpha-particles.

[17] Chao, Lauritsen, and Tollestrup, Phys. Rev. **76**, 586 (1949). Brown, Chao, Fowler, and Lauritsen, Phys. Rev. **78**, 88 (1950).
[18] Van Patter, Sperduto, Strait, and Buechner, Phys. Rev. **79**, 900 (1950).
[19] C. C. Lauritsen and R. G. Thomas, Phys. Rev. **78**, 88 (1950).
[20] Lauritsen, Lauritsen, and Fowler, Phys. Rev. **59**, 241 (1941).
[21] Fowler, Lauritsen, and Lauritsen, Rev. Sci. Instr. **18**, 818 (1947).
[22] A. V. Tollestrup, Phys. Rev. **74**, 1561 (1948).

The gamma-radiation produced during the various bombardments was monitored with a Geiger-Müller counter made by the Radiation Counter Laboratories of Chicago. The wall of the counter was glass weighing 30 mg/cm² and the cathode was a thin silver deposit on the wall. The effective length of the counter was $3\frac{5}{8}$ inches and its diameter was 23/32 inch. The counter was mounted axially in a lead cylinder $2\frac{7}{8}$ inches in diameter with a slot the width and length of the counter cut to admit the radiation. The hole for the counter was lined with an aluminum cylinder whose wall thickness was 3/32 inch.

III. EXCITATION ENERGY OF Li^{7*}

The excitation energy of the state is determined directly by measuring the energies of incident and inelastically scattered protons and solving for the reaction energy Q by the usual formula of nuclear dynamics.[22a] The excitation energy is equal to $-Q^*$, where Q^* applies to the inelastic scattering process in which Li^{7*} is produced. The entire procedure involves three separate measurements. First, the energy scale of the electrostatic accelerator is calibrated. The resulting datum is a conversion factor between the potentiometer reading for the voltage on the electrostatic analyzer and the absolute energy in kev of the bombarding protons. Second, the magnetic spectrometer is calibrated against the electrostatic analyzer. In the present instance, since the magnetometer reading is inversely proportional to the magnetic field of the spectrometer, the resulting datum is a constant which is to be divided by the square of the magnetometer reading to give the energy of the scattered protons. Third, with a fixed bombarding energy, the energy of protons, inelastically scattered from a lithium target, is measured. Details of the calibrations, including small relativistic corrections, are given in Appendix A.

For calibration of the spectrometer, curves which we have termed "profiles" were run for thick targets of copper and lithium and for the thin contamination layers of carbon and oxygen which appear on the surface of the lithium. These profiles are shown in Fig. 1 and Fig. 2. All were taken with a bombarding energy of 1237.3 kev, and observations were made at an angle of 81.1 degrees relative to the beam with the target symmetrically placed relative to incident and outgoing beams. A copper scattering curve using HH^+ ions (mass 2 beam) was also obtained in order to calibrate the spectrometer in the region intermediate between the elastic and inelastic protons scattered by lithium. In the calculations a small correction for surface layer losses was made on E_1. For the thick targets, the magnetometer reading corresponding to the midpoint in the rise for a given group of particles plus a correction

[22a] We have incorporated all mathematical details in the appendices. The expression for Q is given in Appendix A, Eq. (11) and an expression for the difference in two Q-values is given in Appendix C, Eq. (3).

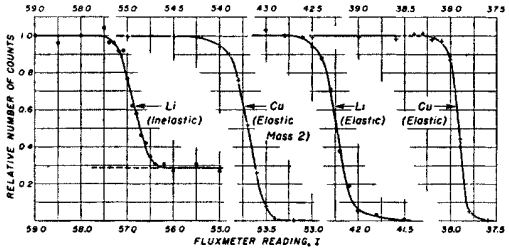

FIG. 1. Spectrometer profiles of the protons scattered at $\theta_{lab}=81.1°$ by thick lithium and copper targets. The energy of the incident protons was 1237.3 kev (618.3 kev for the individual protons in the mass 2 or HH^+ beam), and the energy of the scattered protons is given non-relativistically by $E_0=1738I^{-2}$ Mev, where I is the fluxmeter reading.

for surface layers was taken as a measure of the scattered energy, and for the thin targets, the centroid of the observed particles, plus one-half the surface layer, was used. These procedures are discussed in Appendix B. In addition, a correction for the isotope Li^6 was made in the lithium case. A major uncertainty in the data is the thickness of contamination layers on the surface of the thick targets. This was minimized by making the bombardments as short as possible consistent with good statistics and by using high energy protons which lose relatively little energy in traversing the film. That the error is quite small was attested by the agreement (see Tables I and II of reference 15) between the calculated values of the spectrometer constant for the various scattering targets and scattered beams.

In the detection of the inelastically scattered protons one must use a semi-thin lithium target on a semi-thin backing. By "semi-thin" is meant a thickness measured in energy units that is greater than the resolution width of the spectrometer but much less than the energy of the incident protons. Actually, the backing foil should

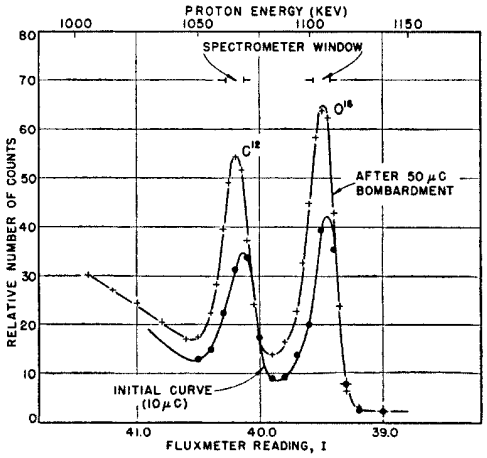

FIG. 2. Spectrometer profiles of the protons scattered at $\theta_{lab}=81.1°$ by thin carbon and oxygen targets. The energy of the incident protons was 1237.3 kev and the energy of the scattered protons is given non-relativistically by $E_0=1738I^{-2}$ Mev, where I is the fluxmeter reading.

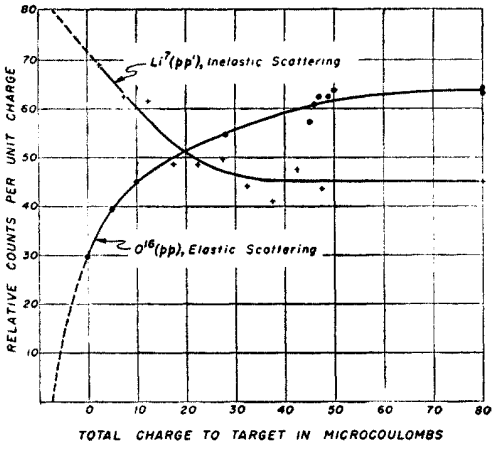

FIG. 3. Dependence of the number of protons scattered by a surface layer of oxygen increasing with amount of bombardment and the corresponding effect on the number of protons inelastically scattered at a given spectrometer setting by the underlying lithium target.

be as thin as possible. The lithium targets were made by evaporation in an "oven" directly below the target chamber and a beryllium foil (~10 kev energy loss for 1 Mev protons) was used as backing. The tail of the elastic scattering from the beryllium and lithium extends, because of straggling and scattering, down to the energy of the inelastic protons, giving a large background count, as is shown by the dashed line in Fig. 1. The background is so large because the cross sections for elastic scattering in lithium and beryllium exceed the lithium inelastic scattering cross section by factors of 10 and 40, respectively. With available foils of higher atomic number than beryllium, the background was found to be even larger.

With the long bombardments required to get sufficient numbers of inelastic protons, the surface contamination became a serious source of error. We were fortunate, however, to be using a target having a smaller atomic number than the contaminants, since this made possible a quantitative evaluation of the error introduced by the surface layers and a correction for it as discussed in the following paragraphs.

First, a preliminary profile curve of the inelastic protons was run. As shown in Fig. 1, its midpoint came at a fluxmeter reading of 56.88 Since this point was reached after considerable bombardment, it was certain that the true midpoint lay somewhat to the right of this one (i.e., at higher energy, smaller fluxmeter reading). Numerous trials with freshly evaporated targets indicated that the midpoint for very short bombardment lay at 56.70. Profile curves of the carbon and oxygen contamination after various lengths of bombardment (Fig. 2) showed definitely that the surface layers increased with bombardment. Consequently, a fresh layer of lithium was deposited, and with the bombarding voltage fixed at 1237.3 kev, points were taken with the spectrometer set alternately at 56.70 (the assumed midpoint for inelastic scattering from lithium) and at 39.50 (the oxygen peak). The latter required only about one-tenth of the bombardment time of the former to give sufficient counts. The resulting data are shown in Fig. 3. As the thickness of the surface layer built up, the lithium profile moved gradually to the left so that the point 56.70 slid gradually down the profile until it reached the background plateau, after which the yield flattened out as shown in the curve. The shape of the two curves was such that extrapolation seemed feasible. It was apparent that a contamination layer existed on the lithium even before the bombardment began. The oxygen curve was therefore extrapolated down to the horizontal axis, and the corresponding value of the extrapolated lithium curve (80 counts per unit charge) was taken as the number of counts which would have been obtained in the absence of any contamination layer. Actually, 80 counts was slightly more than half-way up the edge of the lithium profile curve, and the fluxmeter reading finally decided upon was 56.60, corresponding to a scattered proton energy of 539.3 kev. Putting this value and the bombarding energy 1237.3 kev into the nuclear dynamics equation with the relativistic corrections discussed in the appendices gave for the reaction energy $Q^* = -479.0$ kev.

The validity of the extrapolation was checked by calculating the Q^* in another way. From the oxygen and carbon profiles in Fig. 3 for minimum bombardment, one can calculate, using formulas discussed later in this paper, the number of nuclei in the contamination layer. It was found that the thickness of the minimum layer was $0.42/\cos 50° = 0.65$ kev for the incident protons (1237.3 kev) and $0.75/\cos 50° = 1.16$ kev for the inelastically scattered protons (537.4 kev, corresponding to a magnetometer reading of 56.7). On correcting the two energies by these amounts, the calculated value of Q^* was -479.3. In the calculation of the layer thickness we used the Rutherford scattering formula, so that the agreement is a good check that the scattering cross sections for carbon and oxygen are not markedly different from the Rutherford values at these energies even though reactions other than scattering do occur.

The inelastic scattering energy was also measured at 137.8° to the beam. The observed lithium edge midpoint was 68.0 for approximately the same amount of bombardment as that of the 56.88 point above. The actual

TABLE III. Estimate of errors in the excitation energy of Li^{7*}.

Quantity	Source of error	Direct error	Error in $E_x = \Delta Q$ (kev)
E_1, E_2	Calibration	$\delta E/E = 10^{-3}$	±0.5
	Surface layer	$\delta\xi/\xi = 0.2$	±0.1
E_2	Location of E_{2B}'	$\delta E_2/E_2 = 10^{-3}$	±0.6
θ	Measurement of θ	$\delta\theta = 0.3°$	±0.4
E_x	Statistical	$\Delta E_x/E_x = 10^{-3}$	±0.5
	Final value and probable error		479.0±1 kev

layer thickness was not measured, but assuming it to give the same percentage correction as in the first case, it yielded a value of -479.1 kev for the value of Q, but with considerably greater probable error.

The statistical probable error of the above determinations was reduced, by numerous trials with freshly evaporated targets, to a relative value of 0.1 percent of the final result. There are several systematic errors of this same order of magnitude. They are discussed in detail in Appendix C and are tabulated in Table III. The final result and estimated probable error for the excitation energy of Li^{7*} or for $-Q^*$ of the inelastic scattering process, $Li^7(p,p')Li^{7*}$, is 479.0 ± 1.0 kev.

The most accurate of the recent measurements of the gamma-ray energy (Table I) is 478.5 ± 0.5 kev. Our value of 479.0 ± 1.0 is in substantial agreement with this. Since our value is proportional to the original energy scale calibration of the accelerator, the agreement gives an independent check on this scale. In order

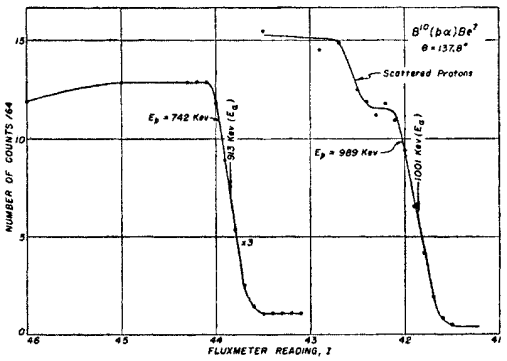

FIG. 4. Spectrometer profiles for the alpha-particles produced at $\theta_{lab}=137.8°$ in the reaction $B^{10}(p,\alpha)Be^7$ by protons of energy 742 kev and 989 kev bombarding a thick B^{10} target. The alpha-particle energy is given non-relativistically by $E_0=1750I^{-2}$ Mev, where I is the fluxmeter reading.

to make the two values coincide, the energy of the $F(p,\alpha'\gamma)O^{16}$ resonance would have to be 872.6 ± 2.0 kev, in agreement within the probable errors with the determination of Herb, 873.5 ± 0.9. We feel that this constitutes an indirect but completely independent check of the current nuclear energy scale.

IV. EXCITATION ENERGY OF Be^{7*}

In order to obtain an accurate value for the difference of the Q-values of the reactions to the ground state and to the excited state of Be^7, the alpha-particles from the two reactions, $B^{10}(p,\alpha)Be^7$ and $B^{10}(p,\alpha')Be^{7*}$, were observed at different bombarding energies, so chosen that the energies of the alpha-particles were approximately the same. In this way the determination of the excitation energy of Be^{7*} was insensitive to errors of calibration of the magnetic spectrometer and to the relatively large energy losses of the alpha-particles in surface layers.

The targets used in this part of the experiment were B^{10} or $(B^{10})_2O_3$ evaporated on aluminum leaf. The B^{10}

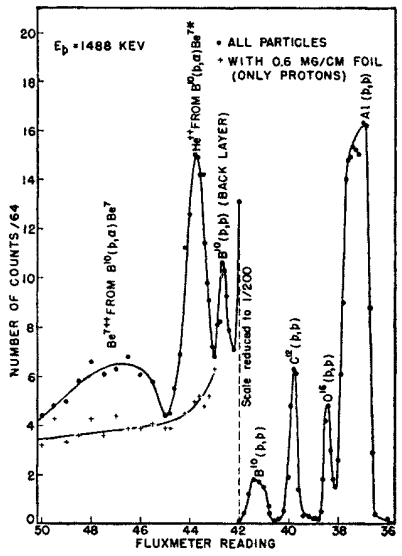

FIG. 5. Spectrometer profiles for alpha-particles, Be^{7++} ions, and scattered protons observed at $\theta_{lab}=137.8°$ from a thin $(B^{10})_2O_3$ target on aluminum bombarded by 1488-kev protons.

isotope was obtained from the Atomic Energy Commission. The target had to be thin enough to keep too many elastically scattered protons and alpha-particles of the main group from deep in the target from entering the spectrometer when the reaction $B^{10}(p,\alpha')Be^{7*}$ was being observed. The subtraction technique, which was used to distinguish between protons and alpha-particles, resulted in large uncertainties whenever the number of protons was equal to or larger than the number of alpha-particles.

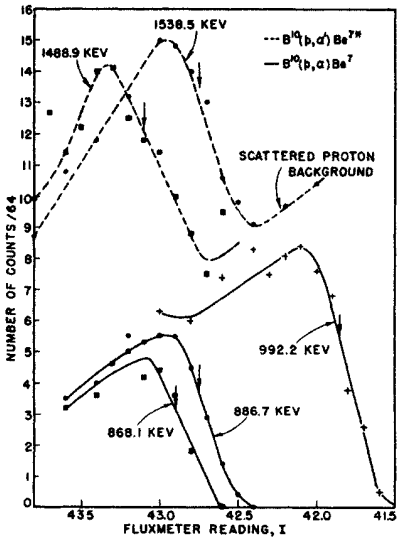

FIG. 6. Spectrometer profiles for the alpha-particles produced in the reactions $B^{10}(p,\alpha')Be^{7*}$ and $B^{10}(p,\alpha)Be^7$ at $\theta_{lab}=137.8°$ by protons of the indicated energies. The target was B^{10} evaporated in a thin layer on Al. The alpha-particle energies are given non-relativistically by $E_0=1750I^{-2}$ Mev, where I is the fluxmeter reading.

TABLE IV. Measurements on the excitation energy of Be^{7*}.

Bombarding proton energy (kev) E_1	E_1'	Fluxmeter reading I	I'	ΔQ (kev)
992.2	1488.9	41.85	43.10	435.4
992.2	1538.5	41.85	42.75	441.0
868.1	1488.9	42.88	43.10	429.7
868.1	1538.5	42.88	42.75	435.2
886.7	1488.9	42.73	43.10	429.8
886.7	1538.5	42.73	42.75	435.3
Mean value and statistical probable error				434.4±3

Profiles of the alpha-particles from the two reactions and of the protons scattered by B^{10}, Al^{27}, C^{12}, and O^{16} are shown in Figs. 4–6. The angle of observation was 137.8°. In Fig. 6 the alpha-particle profiles are shown on an extended inverse momentum scale. In the series of measurements here represented the two alpha-particle groups have about the same energy. It was these measurements which were used to obtain ΔQ, and the results are tabulated in Table IV. The calculation of ΔQ was made using Eq. (3) of Appendix C. An estimate of the target thickness from the shape of the curves indicated that the point which most probably represented the energy of the alpha-particles from the front surface of the target was that at which the yield was 0.6 times the maximum. This choice is particularly uncertain in the case of the alpha-particles accompanying the production of Be^{7*} because of the large background of scattered protons.

Each of the three readings for the main group was combined with each of the two readings for the second group in order to give, as nearly as possible, equal weight to each, and the resulting six values of ΔQ were averaged. The scatter of the results indicates that the statistical probable error of the average is about ±3 kev. This error and the systematic errors are tabulated in Table V. It will be noted that we have estimated a relative error of 0.15 percent for the determination of E_{2B}' and that this contributes the largest part of the systematic error. The final value and probable error for the excitation energy of Be^{7*} is 434.4±4 kev. This is to be compared with other determinations given in Table II and in particular with the value 431±5 kev given by Van Patter, *et al.*[18]

The three determinations of the energies of the alpha-particles from $B^{10}(p,\alpha)Be^7$ can be used to obtain three measurements of the Q of this reaction, and these have been combined with eight determinations by Chao, Lauritsen, and Tollestrup,[17] using the same apparatus and methods as described in this report to yield an average value $Q=1.148\pm0.006$ Mev. This can be combined with our value for the ΔQ to give $Q^*=0.714\pm0.008$ Mev for the $B^{10}(p,\alpha')Be^{7*}$ reaction. These results are to be compared with those of Van Patter, *et al.*[18] which are $Q=1.152\pm0.004$ and $Q^*=0.721\pm0.006$ Mev.

TABLE V. Estimate of errors in the excitation energy of Be^{7*}.

Quantity	Source of error	Direct error	Error in $E_x=\Delta Q$ (kev)
E_1, E_2	Calibration	$\delta E/E=10^{-3}$	±0.4
	Surface layer	$\delta\xi/\xi=0.2$	±0.1
E_2	Location of E_{2B}'	$\delta E_2/E_2=1.5\times10^{-3}$	±2.7
θ	Measurement of θ	$\delta\theta=0.3°$	±0.6
E_x	Statistical	$\delta E_x/E_x=7\times10^{-3}$	±3.0
	Final value and probable error		434.4±4

The average of the two values for $Q=1.150\pm0.003$ can be employed with the value[23] $Q=-1.645\pm0.002$ Mev for $Li^7(p,n)Be^7$ to give a value for the Q of the reaction $B^{10}(n,\alpha)Li^7$ equal to 2.795±0.004 Mev. From this one can calculate that Q^* for $B^{10}(n,\alpha')Li^{7*}$ is equal to 2.316±0.004 Mev, which is in excellent agreement with the value 2.310±0.010 Mev which has been recently determined by careful ionization measurements.[24]

V. THE CROSS SECTIONS

Cross sections were measured as a function of proton energy for the following reaction products: (a) the main group of alpha-particles from $B^{10}(p,\alpha)Be^7$ at 137.8°, (b) the lower energy group of alpha-particles from $B^{10}(p,\alpha')Be^{7*}$ at 137.8°, (c) the gamma-radiation from the decay of the residual Be^{7*} at 90°, (d) the protons elastically scattered by B^{10} at 137.8°, (e) the protons elastically scattered by Li^7 at 81.1° and 137.8°, (f) the protons inelastically scattered at the same angles by Li^7 according to the reaction $Li^7(p,p')Li^{7*}$, and (g) the gamma-radiation from the decay of the residual Li^{7*} at 90°. All the angles listed above are in the laboratory system of coordinates and are measured relative to the direction of the incident proton beam.

(A) The Cross Section of $B^{10}(p,\alpha)Be^7$

The cross section of the main group of alpha-particles was measured for proton energies from 615 kev to 1114 kev and from 1208 kev to 1585 kev. It was necessary to use different target arrangements in the two energy ranges to avoid scattered protons. Between 1114 kev and 1208 kev, with either target arrangement, large numbers of protons were scattered into the spectrometer with energies such as to be counted, and reliable data for the alpha-particles could not be obtained.

For bombarding energies between 615 kev and 1114 kev, the target was made by evaporating on a copper strip a layer of $(B^{10})_2O_3$ thick enough to stop all incident protons. At these bombarding energies, protons scattered elastically by heavy backing material had approximately the same energy as the alpha-particles from the reaction being studied, and it was necessary to absorb them in the target. The upper limit on the bombarding energy was the energy at which the protons scattered

[23] Herb, Snowdon, and Sala, Phys. Rev. 75, 246 (1949). Shoupp, Jennings, and Jones, Phys. Rev. 76, 502 (1949).
[24] Jesse, Forstat, and Sadauskis, Phys. Rev. 77, 782 (1950).

from oxygen had nearly the same energy as did the alpha-particles from the reaction.

In these measurements the energy loss in the target for the reaction products is greater than the energy interval accepted by the spectrometer window. The cross section in the center-of-mass system is thus given by[15]

$$\sigma(\theta_c)=4\pi/\Omega_c(R_c\epsilon_{\text{eff}}/2E_{20})fY(\text{He}^{++}) \quad (5)$$

$$=(R_c\epsilon_{\text{eff}}/q\Omega_cE_{20})fN(\text{He}^{++})\times10^{-3}\text{ barns}, \quad (5')$$

where $\sigma(\theta_c)$ is 4π times the cross section per unit solid angle observed at an angle θ_c in the center of mass coordinates with the incident proton beam. $Y(\text{He}^{++})$ is the number of doubly-charged helium ions observed per incident proton. It is given by $(1/q)N(\text{He}^{++})\times1.602\times10^{-13}$, where $N(\text{He}^{++})$ is the number of doubly-charged helium ions observed for q microcoulombs of protons incident on the target. The factor $f=1+Y(\text{He}^{+})/Y(\text{He}^{++})$ corrects for those helium nuclei which are produced in the reaction but are not counted because they are only singly charged when they leave the target, having captured an electron. The correction for singly-charged helium ions was obtained from a curve prepared by R. G. Thomas of this laboratory using data of Henderson,[25] Briggs,[26] and Rutherford.[27] No correction was made for neutral particles, their number being very small at the energies encountered in these experiments. The quantity $2E_{20}/R_c\epsilon_{\text{eff}}$ is the number of effective target nuclei per square centimeter perpendicular to the beam; this is shown in Appendix B. In (5') $\epsilon_{\text{eff}}=\epsilon_1(\partial E_2/\partial E_1+\eta)$ must be in the customary units, 10^{-15} ev-cm^2 and E_{20} the energy of the observed particles must be in electron-volts; Ω_c is the solid angle in the center-of-mass system in steradians.

The cross section given by Eq. (5) is not the cross section at the energy E_{1B}, of the incident particles leaving the electrostatic analyzer and impinging on the top layer of the target. In Appendix B it is shown that the energy of the incident particles actually producing the observed particles is given by Eq. (3'). In this equation E_{2B} is the energy of the outgoing particles produced when the incident particles do have energy E_{1B}. The quantity E_{2B} can be calculated for each analyzer setting, E_{1B}, from Eq. (12) of Appendix A once the Q of the process has been determined, as by the methods discussed previously in this paper. We have, in general, prepared extensive tables of E_{2B} *vs* E_{1B} as aids during the actual determination of cross section data. The magnetic spectrograph is set at each determination at a "following" energy E_{20}, just enough below E_{2B} to fill the spectrograph window or to avoid surface layer effects. From time to time complete profiles were run to check the entire procedure. As noted above the energy E_1 was determined from the calculated E_{2B}, and the measured values of E_{1B} and E_{20} using (3') of Appendix B.

The solid angle correction from laboratory to center-of-mass coordinates was made according to the following non-relativistic expression:

$$\Omega_c/\Omega\approx d\Omega_c/d\Omega=[(1-\alpha^2\sin^2\theta)^{\frac{1}{2}}+\alpha\cos\theta]^2/(1-\alpha^2\sin^2\theta)^{\frac{1}{2}}\approx1+2\alpha\cos\theta \quad (6)$$

where

$$\alpha=\{M_1M_2E_1/[(M_2+M_3)M_3Q+M_0M_3E_1]\}^{\frac{1}{2}}, \quad (7)$$

Ω is the solid angle of acceptance of the spectrometer, and E_1 is the energy of the bombarding particle in laboratory coordinates at the point where the reaction takes place. It is true that θ_c is a variable depending on E_1 given by

$$\cos\theta_c=\cos\theta(1-\alpha^2\sin^2\theta)^{\frac{1}{2}}-\alpha\sin^2\theta\approx\cos\theta-\alpha\sin^2\theta. \quad (8)$$

The variation is small, however, and the results are essentially the cross section in center of mass coordinates over a range of angles slightly greater than θ, the angle of observation in laboratory coordinates.

The factor R_c/Ω which enters Eq. (5) when (6) is applied, is a constant of the spectrometer and can be determined from any reaction whose cross section is already known. In this case the elastic scattering of 1488 kev protons from copper was used. The cross section was calculated from the Rutherford formula and R_c/Ω was found to be 23,400 steradian^{-1} with a statistical uncertainty of about $\frac{1}{2}$ percent and an uncertainty arising from lack of knowledge of the stopping cross section of copper of about 5 percent.

In measuring the cross section for bombarding energies between 615 kev and 1114 kev numerous complications were encountered because of the background of low energy singly charged alpha-particles produced in deep layers of the target and of protons which had suffered large energy losses in the target (straggling). These backgrounds were assumed to vary slowly with the energy of the observed particles and were evaluated at several bombarding energies by observations at magnetic fields just slightly higher than those at which the He^{++} groups appeared. Correction factors for the penetration of the aluminum foils before the counter by protons and alpha-particles were also determined empirically.

For bombarding energies between 1208 and 1585 kev, the targets were thin layers of $(B^{10})_2O_3$ evaporated on aluminum leaf. The targets were oriented with the $(B^{10})_2O_3$ on the back side of the aluminum, so that both the protons and alpha-particles passed through the aluminum foil. Thus, the alpha-particles appeared with much lower energy than did the scattered protons. The upper limit to the bombarding energy was set by breakdown of the stabilizer of the electrostatic analyzer; the lower limit was the energy at which protons scattered by the boron came from the target with the same energy as the alpha-particles. There were at all bom-

[25] Henderson, Proc. Roy. Soc. (London) **A109**, 157 (1925).
[26] Briggs, Proc. Roy. Soc. (London) **A114**, 341 (1927).
[27] Rutherford, Phil. Mag. **47**, 277 (1924).

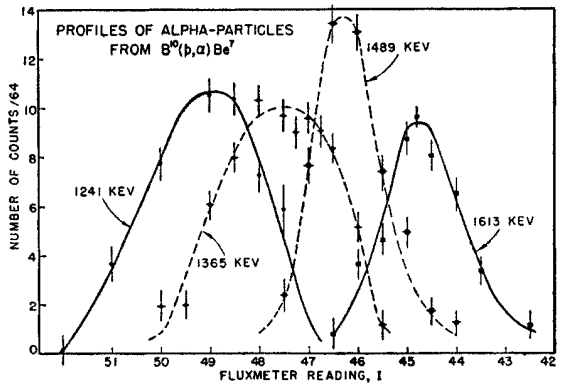

FIG. 7. Spectrometer profiles of alpha-particles observed at $\theta_{lab}=137.8°$ from $B^{10}(p,\alpha)Be^7$ at the bombarding energies indicated. The target was a thin layer of $(B^{10})_2O_3$ on the back side of an 0.2 mg/cm² Al foil.

barding energies some protons of the same energy as the alpha-particles, but at the alpha-particle energies encountered, the aluminum foils in front of the counter could be used to distinguish protons from alpha-particles as long as the protons were not too numerous.

Three runs were made, one with one target set with θ_1 in Fig. 17 equal to 28°, the other two with another target on a thinner aluminum leaf, which was set perpendicular to the proton beam to make the loss of energy by the alpha-particles in the aluminum leaf the same as in the other case. Because the alpha-particles exhibited straggling when they emerged from the aluminum leaf, the spectrometer would not select those from any particular lamina of the target, so all of them produced in the whole target thickness were counted.

Complete profiles were taken at four bombarding energies. These profiles were used to determine the integrals which appear in the cross section for thin

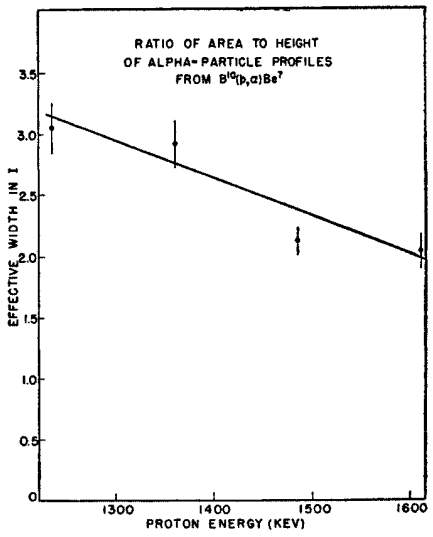

FIG. 8. Effective width of the alpha-particle profiles shown in Fig. 7.

target measurements, which is[15]

$$\sigma(\theta_c)=\frac{4\pi R_c}{nt\Omega_c}\int\frac{fY(\mathrm{He}^{++})}{I}dI \tag{9}$$

$$=\frac{2R_c}{q\Omega_c}\left(\frac{10^{12}}{nt}\right)\int\frac{fN(\mathrm{He}^{++})}{I}dI \text{ barns}, \tag{9'}$$

where $Y(\mathrm{He}^{++})=(1/q)N(\mathrm{He}^{++})\times1.602\times10^{-13}$ is the number of alpha-particles per incident proton counted at a fluxmeter reading I, n is the disintegrable nuclei per cc in the target, and t is the thickness of the target parallel to the incident beam.

At the four bombarding energies chosen, the ratio of the integral in Eq. (9) to the maximum value of the integrand, $fY(\mathrm{He}^{++})/I$, was found, and this ratio was used to find equivalent values of the integral at intermediate bombarding energies from the maximum values of the integrand at those energies. The profiles of the alpha-particles are shown in Fig. 7, and the four points and the curve used for the ratio are shown in Fig. 8. The ratio of the integral to the maximum value of the integrand was used for both targets, although measured for only one, because the energy loss of the alpha-particles was the same for the two targets and the straggling was therefore also the same.

The value of nt used was found from elastic scattering of protons from the B^{10} nuclei, using the proton scattering cross section of boron found as described in part (D) of this section. The two targets were of nearly the same thickness, and the value used for both was 4.18×10^{17} B^{10} nuclei/cm²; the uncertainty in each value was larger than the difference.

It was also necessary to correct the bombarding energy for the energy lost by the protons in passing through the aluminum foil. Using the arguments discussed in Appendix B, one has

$$E_1=E_{1B}-(\epsilon_1/\epsilon_{\mathrm{eff}})(E_{2B}-E_{20}), \tag{10}$$

where E_{1B} = energy of protons from accelerator, E_{20} = energy of alpha-particles observed with B_2O_3 on back side of foil, and E_{2B} = energy of alpha-particles calculated for B_2O_3 on front side of foil using Q from preceding section and the measured E_{1B} in Eq. (12) of Appendix A.

The cross section for $B^{10}(p,\alpha)Be^7$ is plotted as a function of bombarding energy in the laboratory system in Fig. 9. There is, in addition to statistics, an uncertainty of 20 percent in the scale of the ordinate, due principally to poor knowledge of the boron stopping cross section on which nt depends, to statistical uncertainty in the determination of N, to uncertainty in the ratio of the integral in Eq. (9) to the maximum value of the integrand, to uncertainty in background corrections, and to uncertainty in the factor f. When corrected for barrier penetration factors for the incoming protons and outgoing alpha-particles, the excitation curve indi-

cates resonances at 1.0 and 1.5 Mev superimposed on a continuous background.

(B) The Cross Section of $B^{10}(p,\alpha')Be^{7*}$

The target used for the excitation curve was a thin layer of B^{10} evaporated on aluminum leaf. It was necessary that the target be thin in order to keep alpha-particles of the main group and scattered protons from deep in the target from interfering with the observations, and that it be thick enough so that the alpha-particles would fill the spectrometer window. Equation (5) was used to determine the cross section with $Y(He^{++})$ determined by the subtraction technique using a foil before the counter to differentiate protons and alpha-particles. Figure 10 shows the two curves obtained. At proton energies above 1488 kev, some of the alpha-particles were counted through the foils in front of the counter. For the final calculations, the proton counts were considered to be constant above 1488 kev as shown by the dotted portion of the curve. This extrapolation probably indicates too high values for the proton counts so that the calculated cross section may be low, relative to the rest of the curve, by as much as 20 percent.

The composition of the B^{10} target was determined by a comparison of its yield for the alpha-particles from $B^{10}(p,\alpha)Be^7$ at 1488-kev proton energy with that of two $(B^{10})_2O_3$ targets. Since $(B^{10})_2O_3$ evaporates at a few hundred degrees centigrade, presumably little pump oil vapor is decomposed and such a target is fairly pure. The ϵ_{eff} for the B^{10} target was found at one energy in this way. Proton scattering showed that the impurities were principally carbon and oxygen, in large amounts, distributed throughout the target layer. The stopping cross sections of oxygen and carbon vary in the same way with energy, so the target could be considered as B^{10} plus a single contaminant. The effective stopping power of the target for the reaction $B^{10}(p,\alpha')Be^{7*}$ was computed for all of the bombarding energies used. The uncertainty in the composition leads to an uncertainty in ϵ_{eff} of 10 percent.

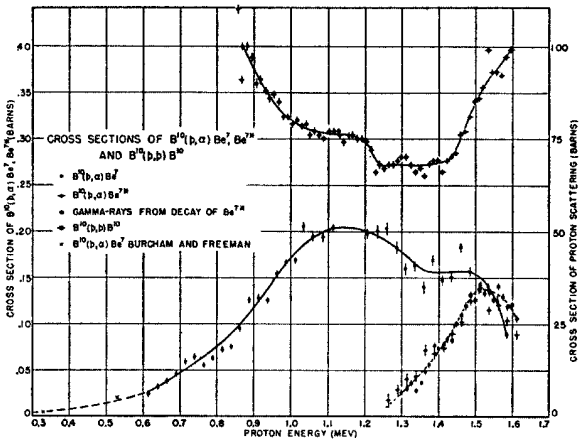

FIG. 9. Cross sections per 4π steradians in the center-of-mass system at $\theta_{cm}\sim140°$ ($\theta_{lab}=137.8°$) for various $B^{10}+H^1$ reactions *vs* laboratory proton energy. The upper curve is for $B^{10}(p,p)B^{10}$; the intermediate curve is for $B^{10}(p,\alpha)Be^7$; the lower curve is for $B^{10}(p,\alpha')Be^{7*}(\gamma)Be^7$. The gamma-rays from the decay of Be^{7*} were measured at $\theta_{lab}=90°$.

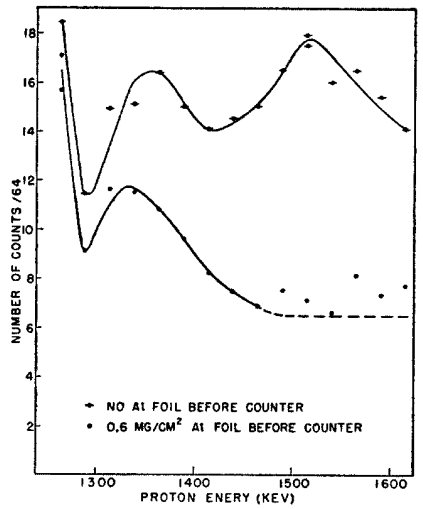

FIG. 10. Curves from which the excitation curve for $B^{10}(p,\alpha')Be^{7*}$ was determined. In the upper curve both scattered protons and the alpha-particles were counted; in the lower curve only the protons were counted.

The curve for the cross section in the center of mass system at $\sim140°$ is shown in Fig. 9 and Fig. 11. In addition to statistics there are the uncertainties in the target composition and the uncertainty in ϵ_{eff}, making the scale of ordinates uncertain by 20 percent. It was remarked earlier that the high energy end of the curve may be low with respect to the remainder of the curve. A marked resonance is indicated near 1.52 Mev with a breadth, $\Gamma\sim250$ kev.

(C) The Cross Section for $B^{10}(p,\alpha')Be^{7*}(\gamma)Be^7$

The gamma-radiation from a B^{10} target bombarded by protons was shown[19] by Lauritsen and Thomas to

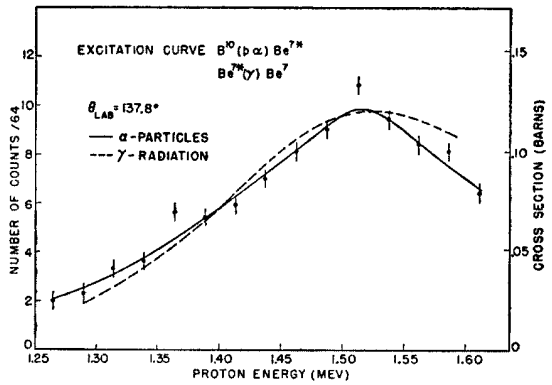

FIG. 11. Cross section per 4π steradians in the center-of-mass system at $\theta_{cm}\sim140°$ ($\theta_{lab}=137.8°$) for $B^{10}(p,\alpha')Be^{7*}$ *vs* laboratory proton energy.

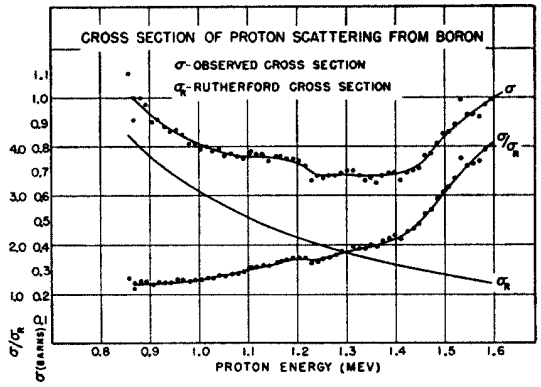

FIG. 12. Cross section per 4π steradians in the center-of-mass system at $\theta_{cm}\sim 140°$ ($\theta_{lab}=137.8°$) for the scattering of protons by B^{10} *vs* the laboratory proton energy. A comparison with Rutherford scattering is shown.

have an energy 429±4 kev, and its origin is thus the decay of the Be^{7*}. Using the techniques described in detail previously,[28] the cross section for this radiation was determined. A thin layer of $(B^{10})_2O_3$ evaporated on copper was used as target.

The thickness of the target was found by a comparison of the yield from the $(B^{10})_2O_3$ target with the differentiated yield from a thick B^{10} target, made by pressing amorphous boron on a copper strip. The thickness of the $(B^{10})_2O_3$ target was found to be 14.1 kev for 1.5-Mev protons, or 1.45×10^{18} boron atoms/cm^2.

The counts arising from background radiation from protons striking the copper target backing were found by measuring the yield from proton bombardment of a copper strip. The background radiation from copper was measured at six proton energies, and the values at intermediate energies were found by graphical interpolation. The background counts were, at most, about 25 percent of the total counts.

The cross section for the gamma-radiation from $B^{10}(p,\alpha')Be^{7*}(\gamma)Be^7$ at 90° to the incident beam is plotted in Fig. 9 and Fig. 11. Uncertainty in the calculated value of target thickness, which depends on the differentiation of a thick target curve and on the stopping cross section of boron and oxygen for protons, makes the scale of the ordinates uncertain by 20 percent. The agreement with the curve for alpha-particles from $B^{11}(p,\alpha')Be^{7*}$ is good, but it is to be noted that the cross section for the gamma-radiation does not fall off as much beyond the peak of the resonance as the cross section for the low energy group of alpha-particles. This may be due entirely to poor extrapolation to high energy of the proton counts in the calculations for the low energy alpha-particles.

(D) The Cross Section for Elastic Proton Scattering by B^{10}

A measurement of the cross section of elastic scattering of protons from B^{10} was made using a thick target made by pressing amorphous B^{10} on a copper

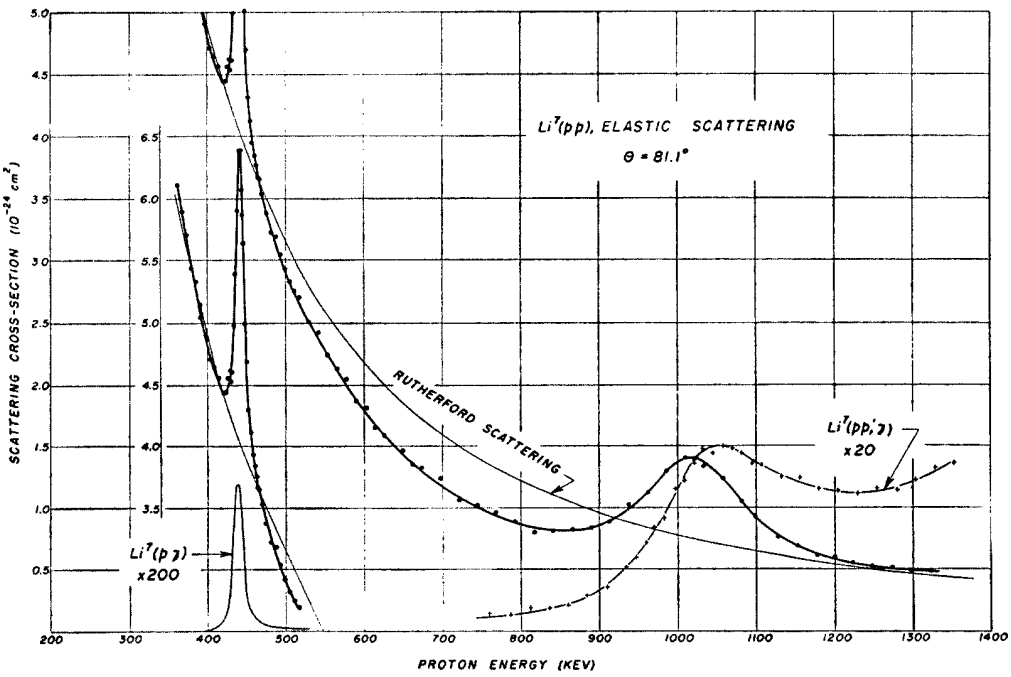

FIG. 13. Cross section per 4π steradians in the center-of-mass system at $\theta_{cm}\sim 85°$ ($\theta_{lab}=81.1°$) for the elastic scattering of protons by lithium. A comparison with Rutherford scattering is shown. It will be noted that anomalies occur at 441 kev, the resonance energy for $Li^7(p,\gamma)$ and near 1050 kev, the resonance energy for $Li^7(p,p'\gamma)$.

[28] Fowler, Lauritsen, and Lauritsen, Revs. Modern Phys. **20**, 236 (1948).

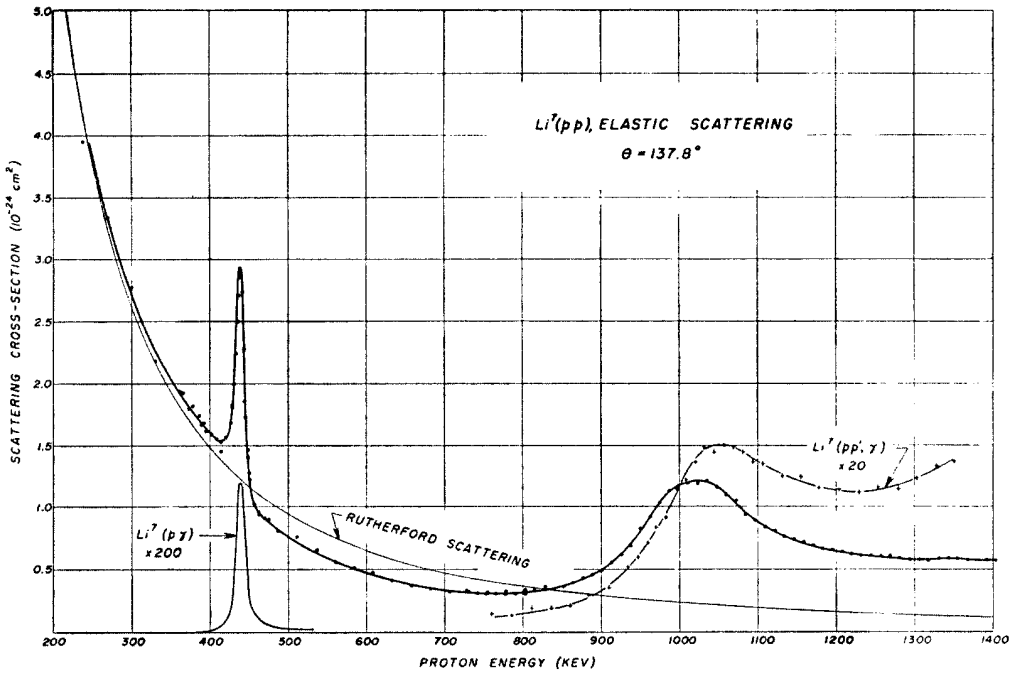

FIG. 14. Cross section per 4π steradians in the center-of-mass system at $\theta_{cm} \sim 145°$ ($\theta_{lab} = 137.8°$) for the elastic scattering of protons by lithium. A comparison with Rutherford scattering is shown. It will be noted that anomalies occur at 441 kev, the resonance energy for $Li^7(p,\gamma)$ and near 1050 kev, the resonance energy for $Li^7(p,p'\gamma)$.

strip. Protons were absorbed in the thick target before being scattered by the copper backing, and it was possible to correct, for the alpha-particles from $B^{10}(p,\alpha)Be^7,Be^{7*}$ produced deep in the target. The alpha-particle cross sections do not change very rapidly with energy, and the alpha-particle counts can be subtracted after measuring them with the spectrometer set for a slightly higher energy than possessed by the scattered protons. Their number was the order of 5 percent that of the number of protons. Again Eq. (5) was used to determine the cross section with $fN(He^{++})$ replaced by $N(H^+)$. No correction was made for neutral hydrogen atoms, their number being very small.

The cross section is plotted in Fig. 9, for comparison with the others, and in Fig. 12, where the ratio to Rutherford scattering is also shown. There is an uncertainty of 10 percent in the scale of ordinates owing principally to ϵ_{eff}. There is a strong anomaly in the neighborhood of the resonances in $B^{10}(p,\alpha)Be^7$ and $B^{10}(p,\alpha')Be^{7*}$ at 1.5 Mev, and a small anomaly at about 1.15 Mev, near the resonance in $B^{10}(p,\alpha)Be^7$.

(E) The Cross Section for Elastic Proton Scattering by Li^7

Measurement of the cross section for the elastic scattering of protons from Li^7 at 81.1° and 137.8° was performed in the manner described in (D) over the energy interval 300 to 1300 kev. Freshly evaporated deposits of lithium (natural isotopic ratio) were used throughout the experiments. The results are shown in Figs. 13 and 14, where the Rutherford scattering is also indicated. It will be noted that a marked anomaly occurs at 441 kev, where $Li^7(p,\gamma)Be^8$ is known to exhibit a strong resonance. This anomaly was first observed by Creutz.[29] Another anomaly will be noted near 1 Mev at which point the inelastic scattering discussed in the next paragraph shows resonance. A detailed discussion of these results will be given in a forthcoming publication after measurements over a wider range of angles have been performed.

(F) The Cross Section for $Li^7(p,p')Li^{7*}$

The cross section for the protons inelastically scattered by Li^7 was measured directly only at a bombarding energy of 1240 kev. The result was 0.036 barn per 4π steradians at 81.1° (laboratory angle) and 0.065 barns per 4π steradians at 137.8° (laboratory angle) in reasonable agreement with the value of 0.057 barns given by the gamma-ray measurements discussed in the next paragraph. The gamma-radiation has been shown to be isotropic by Littauer[30] and thus the gamma-radiation cross section should be equal to the inelastic proton cross section averaged over all angles. We have also observed a large anomaly in the elastic scattering in this region. These observations will be reported at a later date.

[29] E. C. Creutz, Phys. Rev. **55**, 819 (1939).
[30] S. Littauer, Proc. Phys. Soc. (London) **63**, 244 (1950).

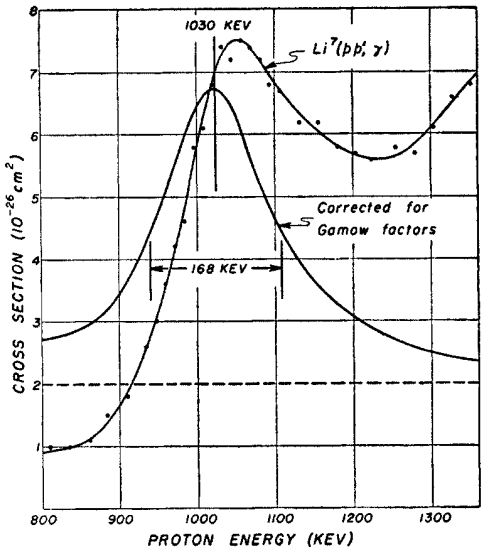

FIG. 15. Excitation curve for gamma-radiation following the inelastic scattering of protons by Li^7.

(G) The Cross Section for $Li^7(pp')Li^{7*}(\gamma)Li^7$

The cross section for the production of the gamma-radiation following the inelastic scattering of protons by Li^7 has been measured at 90° in the laboratory system over the interval of bombarding proton energies from 800 to 1400 kev. The results are shown in Fig. 15 where we also show the cross section corrected for the barrier penetration factors[31] for the incoming and inelastically scattered protons. This curve indicates a resonance at 1030±5 kev with a full width at half-maximum of 168 kev superimposed on a relatively constant background. The thick target yield (92.6 percent Li^7) was measured at 1350 kev and was found to be 1.2×10^{-5} quanta/proton.

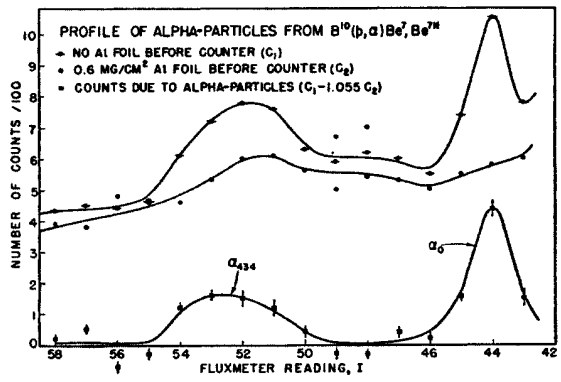

FIG. 16. Alpha-particle groups observed at $\theta_{lab}=137.8°$ from the bombardment of B^{10} by 1460 kev protons. A thin layer of $(B^{10})_2O_3$ evaporated on the back side of a thin Al leaf was used as the target. The groups corresponding to the formation of Be^7 in the ground and 434-kev states are evident. No evidence for a group leaving Be^7 in a state at 205 kev is indicated.

[31] R. F. Christy and R. Latter, Revs. Modern Phys. **20**, 185 (1948).

VI. OTHER ENERGY LEVELS OF Be^7 AND Li^7

When Grosskreutz and Mather reported the existence of a state at about 470 kev from studies of $Li^7(p,n)Be^7$ at 5.1 Mev, they also reported two additional excited states of Be^7, at 205±70 kev and at 745±70 kev above the ground state. Previously, Mandeville, Swann, and Snowdon[32] had concluded that no state between 0.5 and 1.0 Mev was excited in $Li^6(d,n)Be^7$ in as much as 10 percent of the disintegrations. After Grosskreutz and Mather announced their results, the levels were looked for by others. The work of Johnson, Laubenstein, and Richards, Hamermesh and Hummel, and Van Patter, Sperduto, and Buechner, and Keepin, yields no evidence from the existence of these levels. (See Table II for references.)

A search was made for alpha-particles from $B^{10}(p,\alpha)Be^{7*}$ leaving the Be^{7*} excited by approximately 200 kev. The target was a thin layer of $(B^{10})_2O_3$ on the back side of an aluminum leaf. The proton energy was 1.46 Mev at the $(B^{10})_2O_3$ layer. The data obtained are shown in Fig. 16, where the indicated errors are those due to statistics. None of the alpha-particles had enough energy to be counted through the aluminum foils in front of the counter. The energies at which the groups of alpha-particles appeared agree with calculations based on the foil thickness. The data indicate that in the reaction $B^{10}(p,\alpha)Be^7$ at a proton energy of 1.46 Mev, the residual Be^7 is not left in any excited state near 200 kev as much as one-tenth as often as in either the ground state or the state at 434 kev. Excitation of the state at 745 kev was not attempted, since if the state exists, the barrier penetration factor for the alpha-particles would be so low that the reaction could not have been observed at the proton energy available. It must be pointed out that Grosskreutz and Mather used proton energies of 5.1 Mev, which is higher than employed by other investigators. All that is indicated by the null results here reported is a choice of two possibilities; either the state does not exist or it cannot be produced in the range of excitations available in these experiments.

Careful studies of the reactions $Be^9(d,\alpha)Li^7$ by several investigators[33] have revealed no additional states in Li^7 up to 2-Mev excitation energy. The next known state in Li^7 occurs at an excitation of 7.38 Mev and was first observed as a resonance[34] at $E_n=0.27$ Mev in $Li^6(n,\alpha)H^3$. The mirror state has been recently found in Be^7 at 7.1 Mev from resonances[35] in $Li^6(p,\alpha)He^3$ and $Li^6(p,p)Li^6$.

VII. CONCLUSIONS

From these experiments it is concluded that there exist excited states in Li^7 and Be^7 at 479.0±1 kev and

[32] Mandeville, Swann, and Snowdon, Phys. Rev. **76**, 980 (1949).
[33] W. W. Buechner and E. N. Strait, Phys. Rev. **76**, 1547 (1949). D. R. Inglis, Phys. Rev. **78**, 104 (1950).
[34] Goldsmith, Ibser, and Feld, Revs. Modern Phys. **19**, 259 (1947) quotes unpublished results of Blair, *et al.*
[35] Bashkin, Ajzenberg, Browne, Goldhaber, Laubenstein, and Richards, Phys. Rev. **79**, 238 (1950).

434.4±4 kev, respectively, and no evidence for additional low-lying states has been found. Additional states do not exist or *they cannot be excited* in the reactions used in these experiments with available excitations. The Q-value for $B^{10}(p,\alpha)Be^7$ has been measured as 1.148±0.006 Mev and for $B^{10}(p,\alpha')Be^{7*}$, as 0.714 ±0.008 Mev.

For the reaction $Li^7(p,n)Be^7$, the Q-value is −1.645 ±0.001 Mev and thus, using $M(n)-M(H^1)=0.782$ ±0.001 Mev,

$$\delta Mc^2=[M(Be^7)-M(Li^7)]c^2=0.863\pm0.002 \text{ Mev}$$
$$\delta M^*c^2=[M(Be^{7*})-M(Li^{7*})]c^2=0.818\pm0.004 \text{ Mev}$$

$\delta(M-M^*)c^2=479-434$ kev$=45\pm4$ kev.

The difference in the splitting of the Be^7 levels and the Li^7 levels is more than ten times the error of measurement and amounts to about 10 percent of the energy splitting between the excited and ground states. There is now considerable evidence for the assumption that the excited state in Li^7 (and presumably in Be^7) has $I=\frac{1}{2}$ forming a ^2P-doublet with the ground state for which $I=\frac{3}{2}$ by direct measurement. This evidence is given by the γ-α angular correlation measurements[36] in $B^{10}(n,\alpha')Li^{7*}(\gamma)Li^7$ and the angular distribution measurements[30] in $Li^7(p,p')Li^{7*}(\gamma)Li^7$. The observed splitting difference reported here is of considerable significance in connection with this probable doublet structure. The over-all separation of the levels is perhaps to be attributed to a new term in the ultimate nuclear forces, such as seems to be manifest in the *jj*-coupling shell model for medium and heavy nuclei, and in the spin-orbit forces of Case and Pais.[7] However, the splitting *difference* in these mirror levels must be sought in terms of electrostatic and magnetic effects, it not being possible to neglect the latter in calculating the small difference.

The matter is discussed in the following paper[7a] by Inglis who first calculated[6] the magnetic contributions to nuclear energies. In regard to the electrostatic effects, it can be expected that the excited states will have slightly larger radii than do the ground states, thus reducing their first-order electrostatic energy difference ($\sim 1/R$). However, a reasonable estimate based on Feenberg's analysis[37] of nuclear compressibility yields $\delta R/R\sim 0.2$ percent and a splitting difference of at most 3 kev. It also can be expected that the larger radii of the Be^7 states relative to the Li^7 states arising from their larger positive electrostatic energies would reduce any reasonable spin-orbit interaction ($\sim 1/R^3$). According to Inglis, a reasonable estimate of the two terms together yields only 10 kev. Furthermore, it does not seem reasonable to ascribe large differences between the ground and excited states to the $\langle 1/r\rangle$ term in Eq. (2). Some contribution to the difference must then arise from the magnetic effects, and in his paper Inglis finds a reasonable agreement between the theoretical expectations and the observed value. Rough agreement is obtained by the use of Eq. (4). It is to be emphasized that the sign (and magnitude) of the separation is correct for $I^*=\frac{1}{2}$ while the sign is given incorrectly, for example, for $I^*=5/2$ in a ^2D-doublet with $I=3/2$.

The calculations lend considerable support to the belief that the excited states in Be^7 and Li^7 at 434 and 479 kev are "mirror" states. Their displacement by the order of 10 percent of their excitation energy indicates that the experimental identification of mirror states may require considerable care and study. At high excitations the mean separation of protons may change substantially, giving large differential electrostatic effects, and for states with high enough energy of excitation to be subject to decay by proton or neutron emission, there may be a considerable displacement ($\sim$1 Mev) of the relative position of the states. A detailed discussion of this effect in the $N^{13}-C^{13}$ case will be published in the near future by R. G. Thomas of this laboratory.

It will remain for additional experimental evidence to confirm in a variety of cases the correspondence of the excited states of mirror nuclei. As indicated in the paper by Inglis, it may be necessary to make detailed calculations of fine structure effects, such as electrostatic and magnetic contributions to the energy of the state, in order to clarify apparent deviations in the excitation energies. Just the fact that a reasonable calculation involving a few tens of kilovolts can be made with some confidence in the case of Be^{7*} and Li^{7*}, constitutes substantial evidence for the equality of the nuclear *pp* and *nn* forces within very narrow limits.

VIII. DISCUSSION OF THE $B^{10}(p,\alpha)Be^7$ CROSS SECTIONS

The $B^{10}(p,\alpha)Be^7$ cross sections measured in these experiments have some bearing on the important question of the spin of the excited states of Be^7 and Li^7. The analysis of the cross section requires first the elimination of barrier factor effects for the incoming protons and outgoing alpha-particles. This has been done by one of us.[38] The analysis indicates that there is probably a resonance in $B^{10}(p,\alpha)Be^7$ at 1.0 Mev superimposed on a broad continuous background extending over the entire range of excitations used in these experiments. The yields are consistent with reasonable values ($\sim$1 Mev) for the widths without barrier of both the protons and alpha-particles on the assumptions that the background arises from *s*-wave capture into a broad state of C^{11} with $I=5/2^+$ and that the resonance arises from *p*-wave capture into a state of C^{11} with $I=3/2^-$. The assumption of $I(Be^{7*})=1/2^-$ along with $I(B^{10})=3^+$ makes it reasonable that the

[36] B. Rose and A. R. W. Wilson, Phys. Rev. **78**, 68 (1950).
[37] E. Feenberg, Revs. Modern Phys. **19**, 239 (1947).
[38] A. B. Brown, PhD. thesis "Excited states of the mirror nuclei, Be^7 and Li^7," California Institute of Technology (1950).

yield of the low energy alpha-particles should be very small in this region since the angular momentum of the outgoing α'-particle must be large, and the barrier factors markedly reduce the yield. On the other hand, the resonance yield for $B^{10}(p,\alpha')Be^{7*}$ at 1.5 Mev is anomalously large compared to $B^{10}(p,\alpha)Be^{7}$ in the same way that the slow neutron yield for $B^{10}(n,\alpha')Li^{7*}$ is large compared to that for $B^{10}(n,\alpha)Li^{7}$.[39] Only for f-wave capture of protons into a C^{11} state with $I=1/2^-$ is the emission of the α' favored (s-wave) by barrier factors over that for the α (d-wave), and in this case the detailed calculations indicate an impossibly large and unobserved partial width for the proton scattering. In the case of s-capture into a C^{11} state with $I=7/2^+$, or of p-capture into $I=5/2^-$, the outgoing waves can have the same minimum value (f and d, respectively), and the widths without barrier for α' are about 10 times those for α. It is true that this factor can be reduced by assuming $I(Be^{7*})=5/2$ or $7/2$, but it must be emphasized that we have found just such variations in widths without barrier in a considerable number of cases of proton induced reactions.[28] Furthermore, considerable confidence is lent to the assignment $I(Be^{7*})=1/2^-$ by the relative yields in the region below 1.3 Mev where, as expected on this assignment, the reaction $B^{10}(p,\alpha')Be^{7*}$ is highly improbable.

In conclusion, we wish to thank Sylvan Rubin and C. Y. Chao, who aided in many of the observations reported here, and R. F. Christy for valuable discussions of the theoretical aspects. We are grateful to D. R. Inglis for communication of his results prior to publication.

APPENDIX A. METHODS OF CALCULATING NUCLEAR Q-VALUES

In the experiments described in this report the excitation energies of Li^{7*} and Be^{7*} are essentially determined as the differences in the Q-values for reactions in which the ground states and excited states are involved. The experiments thus reduced to the determination of reaction Q-values. In the lithium case in which the reactions are the special cases of scattering, the Q-value of one of the processes, the elastic scattering, is of course equal to zero, and some advantage can be taken of this fact in ascertaining the over-all accuracy of the methods employed. In this appendix we discuss certain points involved in the accurate determination of the release of energy in nuclear reactions. In addition to a general treatment of the methods of calculating Q-values from the experimental data, we wish to consider small effects arising from special relativity, from thermal motion of the target nuclei, and from the choice of masses—nuclear, atomic, or integral. In Appendix B we consider the effects of energy losses and straggling in the target material and in surface contamination layers. In Appendix C we attempt to ascertain the error produced in the final result by errors made in the evaluation of the directly determined quantities. Throughout these appendices we calculate, as examples, appropriate correction terms, δQ, to illustrate the order of magnitude of the corrections necessary to account for small effects. In actual calculations we have applied the corrections straight-forwardly in an exact manner.

The Q-value of a nuclear reaction is by definition the difference in rest mass in energy units of the initial and final nuclei involved. For two initial and two final nuclei this becomes:

$$Q=(M_0+M_1-M_2-M_3)c^2, \tag{A1}$$

where we use the usual subscript notation, *zero* for the target nucleus, *one* for the bombarding particle, *two* for the observed particle, and *three* for the residual nucleus or particle. To avoid duplication, we do not use an additional subscript to designate rest mass when a subscript is already employed to identify the mass. Strictly, it is only correct to use nuclear masses in (A1), but atomic masses can be used if positron emission is not involved and if electronic binding energies are neglected. The neglect of electronic binding energies involves an error in Q if calculated from atomic masses of the order of

$$\delta Q\approx 36(Z_0+Z_1)^{4/3}(Z_1-Z_2)\text{ ev} \tag{A1'}$$

for $Z_0>Z_1$ and $Z_3>Z_2$. If atomic masses are employed in (A1) then Q should be replaced on the left-hand side by $Q+\delta Q$ with δQ given by (A1'). To derive (A1') we employ $E_b\approx 15.6Z^{7/3}$ ev as a rough estimate of total atomic binding energies. The error is -0.4 kev for the reaction $B^{10}(p,\alpha)Be^{7}$, for which $Z_0+Z_1=6$ and $Z_1-Z_2=-1$. In general, the masses are not known accurately enough to make any correction necessary. In the experiments described here the determination of Q from mass spectroscopic values is not possible at the present time, and nuclear methods must be employed. When Q-values determined by nuclear methods are employed to determine an unknown *atomic* mass from known ones, the Q-value should first be corrected by a small amount equal to that given by (A1').

The determination by nuclear methods[40,41] depends on the expression:

$$Q=E_2+E_3-E_0-E_1=E_2+E_3-E_1, \tag{A2}$$

where the E's designate kinetic energies. This can be derived from (A1) by using the conservation of the total energy, mass plus kinetic, before and after the reaction. It will be noted that (A2) is relativistically correct. In the second equality we neglect the thermal energy of the target nuclei. This is certainly valid in Eq. (A2) since $E_0\sim 0.025$ ev at ordinary temperatures, and at the present time, under the best circumstances, it is not possible to reduce errors in the measurement of E_1, E_2, and E_3 to less than several hundred electron volts. The determination of Q thus can be reduced to the determination of the energies E_1, E_2, and E_3. In actual practice the energy of only one of the outgoing particles is measured directly and that of the other is calculated using the conservation of momentum.

In the most accurate early investigations the energy of the incident particle was determined by a direct measurement of the high potential on the accelerating device. The energy of the emitted particle was usually determined by range or ionization measurements. Recently, these methods have been supplanted by the use of electrostatic,[42] velocity,[43] and magnetic[44] analyzers or spectrometers. For energies exceeding 1 Mev, direct measurements of the accelerating potential are impractical, and range measurements have not proven sufficiently precise, the accuracy being limited to $\sim$1 percent. In the experiments described in this paper a 90° cylindrical electrostatic analyzer[42] has been used to measure E_1, and a 180° double focusing magnetic spectrometer[44] has been used to measure E_2.

[39] D. R. Inglis, Phys. Rev. 74, 1876 (1948).

[40] M. S. Livingston and H. A. Bethe, Revs. Modern Phys. 9, 245 (1937).

[41] C. E. Mandeville, J. Franklin Inst. 244, 385 (1947).

[42] Allison, Frankel, Hall, Montague, Morrish, and Warshaw, Rev. Sci. Instr. 20, 735 (1950); Herb, Snowdon, and Sala, Phys. Rev. 75, 246 (1949); Fowler, Lauritsen, and Lauritsen, Rev. Sci. Instr. 18, 818 (1947).

[43] Shoup, Jennings, and Jones, Phys. Rev. 76, 502 (1949).

[44] Snyder, Rubin, Fowler, and Lauritsen, Rev. Sci. Instr. 21, 852 (1950); Burcham and Freeman, Phil. Mag. 40, 807 (1949); Buechner, Strait, Stergiopoulos, and Sperduto, Phys. Rev. 74, 1569 (1948).

The Electrostatic Analyzer

In an electrostatic analyzer the "electric rigidity" of the particle trajectory (field×radius of curvature) is used as a measure of the particle's energy. The kinetic energy of the particle is given relativistically by

$$E=E_0-M_0c^2+(M_0^2c^4+E_0^2)^{\frac{1}{2}} \approx E_0(1+E_0/2M_0c^2) \quad \text{for} \quad E_0\ll M_0c^2. \tag{A3}$$

Here E_0 is the energy calculated on the basis of simple proportionality to the centrifugal force and thus to the measured potential V across the analyzer plates (symmetrically charged). It is given by

$$E_0=\tfrac{1}{2}Mv^2=E(M_0c^2+\tfrac{1}{2}E)/(M_0c^2+E)=ZeV/2\ln(\rho_1/\rho_2) =ZeV\rho/2d[1+(1/24)(d^2/\rho^2)+\cdots]\approx ZeV\rho/2d=C_eZR. \tag{A4}$$

In Eq. (A4), ρ_1 and ρ_2 are the radii of the plates, $d=\rho_1-\rho_2$ is the plate separation, and $\rho=(\rho_1\rho_2)^{\frac{1}{2}}$ is the geometric mean of the radii of curvature. Ze, M_0, and P are the charge, rest mass, and momentum of the particle, respectively. R is the reading of the device by which V is measured, usually a potentiometer across a portion of the plate resistor stacks, and C_e is a constant of the apparatus. Small corrections for edge effects, misalignment of entrance and exit slits, superimposed magnetic fields, and other factors have been adequately discussed previously.[42a, b] The focal properties which make energy measurements with the analyzer independent of the entrance angle in the plane of curvature and of the angle of deflection have also been completely treated. In the experiments described here the constant C_e was determined by measurements on the strong gamma-ray resonance in the reaction $F^{19}(p,\alpha\gamma)$ at a proton energy of 873.5 kev.[42] Rough measurements of ρ and d checked the value obtained. The linearity was checked by measurements on H^+, HH^+, and HHH^+ ions using for detection a magnetic spectrometer at a fixed field setting. Relativistically correct results were given conveniently by using the approximate form of (A3). Numerically, for R in millivolts and E_0 in Mev, $C_e=0.12368$.

The Magnetic Spectrometer

In a magnetic spectrometer the "magnetic rigidity" is measured and gives directly the relativistically correct momentum of the particle. The energy is thus given by

$$E=(M_0^2c^4+2E_0M_0c^2)^{\frac{1}{2}}-M_0c^2 \approx E_0(1-E_0/2M_0c^2) \quad \text{for} \quad E_0\ll M_0c^2 \tag{A5}$$

where E_0 is the energy calculated on the basis of a simple quadratic dependence on the measured magnetic induction B. It is given by

$$E_0=P^2/2M_0=(B\rho Ze)^2/2M_0c^2=0.4827(ZB\rho)^2/M_0\times10^{-10}\ \text{Mev} =C_mZ^2/M_0I^2. \tag{A6}$$

The numerical value is for $B\rho$ in gauss-cm and M_0 in atomic mass units. Here I is the reading of a fluxmeter of the type used for some time in this laboratory.[45] The constant C_m was determined by measurements on particles of known energy after scattering off targets of Li, Be, C, O, Al, Cu, and Au. Linearity in I^{-2} was checked by measurements on H^+, HH^+, and HHH^+ ions of the same energy as determined by the electrostatic analyzer at a fixed setting. Relativistically correct results were given conveniently by using the approximate form of (A5). Numerically, $E_0=1738I^{-2}$ Mev for protons and $E_0=1750I^{-2}$ Mev for alpha-particles. These expressions hold for I in the units used in all of the figures of this paper.

Equations for Q

As noted previously, only one of the energies, E_2 and E_3, is measured directly, and usually the energy of the lighter particle is measured rather than that of the heavier. In general, this gives the higher precision in the final result although, if the emitted particle is a neutron, more precise results may be obtained by measurements on the other nucleus which, because of its charge, can be deflected in a magnetic or electric field. In any case, the energy not measured directly is determined by measuring the angle of emission, θ, with the direction of bombardment as well as the energy of the one product and then using the relativistically correct expression for the conservation of momentum in the over-all process, namely

$$P_3^2=P_2^2-2P_2P_1\cos\theta+P_1^2. \tag{A7}$$

Here θ is the angle of emission of particle 2 with the original direction of particle 1. In writing Eq. (A7) we have neglected P_0, the momentum of the target nucleus arising from its thermal motion. It is true that this motion will cause an observed spread[46] in either P_2 or P_3 at any given angle of observation. However, if we employ appropriately averaged values of P_2 and P_3 in Eq. (A7), we can neglect terms in P_0. This is because terms linear in P_0 yield zero when averaged over all possible directions of motion, and those quadratic in P_0 are of the order of $E_0=0.025$ ev and are thus negligible.

At this point it is usually considered sufficiently accurate in the customary Q-value determinations to employ the non-relativistic relation between the energy, momentum, and rest mass of each particle, namely:

$$P^2=2EM_0. \tag{A8}$$

Upon substitution of (A8) in (A7) one obtains

$$E_3=(M_2E_2/M_3)+(M_1E_1/M_3)-2\mathcal{E}\cos\theta, \tag{A9}$$

where

$$\mathcal{E}=(M_1M_2E_1E_2/M_3^2)^{\frac{1}{2}}. \tag{A10}$$

Then using (A2),

$$Q=\frac{M_3+M_2}{M_3}E_2-\frac{M_3-M_1}{M_3}E_1-2\mathcal{E}\cos\theta, \tag{A11}$$

or

$$Q=\frac{M_3+M_2}{2M_3M_2}P_2^2-\frac{M_3-M_1}{2M_3M_1}P_1^2-\frac{1}{M_3}P_1P_2\cos\theta, \tag{A11'}$$

and in a convenient form for application in the experiments described in this report

$$Q=\frac{M_3+M_2}{2M_3M_2}P_2^2-\frac{M_3-M_1}{M_3}E_1-\frac{1}{M_3}(2M_1E_1)^{\frac{1}{2}}P_2\cos\theta. \tag{A11''}$$

Equation (A11) can be solved for E_2 as a function of E_1, Q, and θ to yield

$$E_2^{\frac{1}{2}}=\frac{(M_1M_2E_1)^{\frac{1}{2}}}{M_2+M_3}\cos\theta \pm\left(\frac{M_3}{M_2+M_3}Q+\frac{M_3-M_1}{M_2+M_3}E_1+\frac{M_1M_2}{(M_2+M_3)^2}E_1\cos^2\theta\right)^{\frac{1}{2}}. \tag{A12}$$

In (A12) the negative sign is only used when the first term is numerically larger than the second and in this case E_2 is a double-valued function of θ, and the angle within which the particle can be observed is limited to a value less than 90°. A form involving $\sin^2\theta$ in the second bracket can be derived using $M_0+M_1\approx M_2+M_3$, but the approximation is of the same order as certain relativistic corrections to be considered later.

Dependence of Q on the Independent Variables

In our further discussion we will be interested in $\delta Q=\Sigma_X(\partial Q/\partial X)\delta X$, where X represents the independent variables

[45] C. C. Lauritsen and T. Lauritsen, Rev. Sci. Instr. **19**, 916 (1948).

[46] In the most common cases where $(M_2+M_3)M_3Q>(M_1M_2-M_0M_3)E_1$, it can be shown that the full spread in E_2 for a given target energy E_0 is given by

$$\delta E_2=4(M_2M_0/M^2)^{\frac{1}{2}}E_0E_2.$$

For the reaction $B^{10}(p,\alpha)Be^7$ this yields $\delta E_2=0.5$ kev when the alpha-particles are observed with $E_2=2$ Mev and when one takes $E_0=0.025$ ev.

in (A11), (A11′), or (A11″) and thus we will need the following partial derivatives:

$$\frac{\partial Q}{\partial \theta}=2\mathcal{E}\sin\theta\rightarrow 2\mathcal{E} \text{ at } 90°, \tag{A13}$$

$$\frac{\partial Q}{\partial E_1}=-\frac{M_3-M_1}{M_3}-\frac{\mathcal{E}}{E_1}\cos\theta\rightarrow-\frac{M_3-M_1}{M_3} \text{ at } 90°, \tag{A14}$$

and

$$\frac{\partial Q}{\partial E_2}=\frac{M_2+M_3}{M_3}-\frac{\mathcal{E}}{E_2}\cos\theta\rightarrow\frac{M_2+M_3}{M_3} \text{ at } 90°. \tag{A15}$$

If the energies are determined we have from (A11)

$$\frac{\partial Q}{\partial M_1}=\frac{E_1}{M_3}-\frac{\mathcal{E}}{M_1}\cos\theta\rightarrow\frac{E_1}{M_3} \text{ at } 90°, \tag{A16}$$

$$\frac{\partial Q}{\partial M_2}=\frac{E_2}{M_3}-\frac{\mathcal{E}}{M_2}\cos\theta\rightarrow\frac{E_2}{M_3} \text{ at } 90°, \tag{A17}$$

and

$$\partial Q/\partial M_3=-E_3/M_3. \tag{A18}$$

If the momenta are determined we have from (A11′)

$$\partial Q/\partial M_1=E_1/M_1, \tag{A16′}$$

$$\partial Q/\partial M_2=-E_2/M_2, \tag{A17′}$$

and

$$\partial Q/\partial M_3=-E_3/M_3. \tag{A18′}$$

From (A12)

$$\frac{\partial E_2}{\partial \theta}=-\frac{2M_3\mathcal{E}\sin\theta}{M_2+M_3-(M_3\mathcal{E}/E_2)\cos\theta}\rightarrow-\frac{2M_3}{M_2+M_3}\mathcal{E} \text{ at } 90°, \tag{A19}$$

$$\frac{\partial E_2}{\partial E_1}=\frac{M_3-M_1+(M_3\mathcal{E}/E_1)\cos\theta}{M_2+M_3-(M_3\mathcal{E}/E_2)\cos\theta}\rightarrow\frac{M_3-M_1}{M_2+M_3} \text{ at } 90°, \tag{A20}$$

and

$$\frac{\partial E_2}{\partial Q}=\frac{M_3}{M_2+M_3-(M_3\mathcal{E}/E_2)\cos\theta}\rightarrow\frac{M_3}{M_2+M_3} \text{ at } 90°. \tag{A21}$$

The Relativistic Solution for Q

In seeking a relativistic solution for Q we must use instead of (A8) the relativistic relation

$$P^2=2EM_0+E^2/c^2. \tag{A8′}$$

An explicit solution using (A8′) involves algebraic expressions of considerable complexity.[47] It will be noted, however, that (A8) is identical with (A8′) if M_0 in (A8) is replaced by an effective mass given by

$$M_{\text{eff}}=M_0+E/2c^2. \tag{A8″}$$

The derivation of (A9), (A11), and (A12) will be as before but with each mass replaced by this effective mass. *Thus the usual non-relativistic expressions involving nuclear Q values can be employed relativistically if only each mass involved is replaced by its effective value which is the rest mass plus one-half the kinetic energy in mass units.* It will be noted that this effective mass is not the relativistic total mass corresponding to the rest mass plus all of the kinetic energy in mass units. It is true that one does not obtain an explicit solution for Q since the effective value of M_3 and thus E_3 appears in (A11). However, when the relativistic corrections are small it is sufficiently accurate to estimate E_3 non-relativistically from (A9), and even for large relativistic effects the method of successive approximations, using (A8″), (A9), (A10), and (A11) is often convenient. When quanta are involved, as in photoeffect reactions and capture-radiation reactions, the substitution $Mc^2=h\nu/2$ makes possible the direct use of these equations.

It is possible to estimate relativistic and other small corrections by using the appropriate partial derivations from (A13) to (A18′). There are three relativistic effects to be taken into account; first, in the determination of the incident particle energy; second, in the determination of the observed emitted particle energy; and third, in the dynamical equation for the Q-value. We calculate $\delta Q=\Sigma_X(\partial Q/\partial X)\delta X$, where X runs through E_1, E_2, M_1, M_2, and M_3, as an example. We obtain the δE from (A3) or (A5) and set each $\delta M=E/2c^2$. The relativistic corrections are then combined into an over-all correction factor, δQ, which will, in general, depend on the methods of energy determination and on the angle of observation. If the energies are known correctly and it is wished to estimate the relativistic correction necessary if rest masses are used in (A11), then the result is particularly simple for 90° observation being given by

$$\delta Q=(E_1^2+E_2^2-E_3^2)/2M_3c^2, \tag{A22}$$

or for large $Q\approx E_2+E_3\gg E_1$

$$\delta Q/Q\approx Q(M_3-M_2)/2M_3c^2(M_3+M_2). \tag{A22′}$$

This was first shown by Livingston and Bethe.[40] In general, the correction is at most of the order of 0.1 percent. Another case is of special interest. If the particle momenta are determined in a relativistically correct manner, as by the use of magnetic analyzers for *both* incoming and outgoing particles, then the momentum of the residual nucleus is correctly given by (A3). The error in a non-relativistic calculation involves only the E-values used in (A2). Hence, the correction to be made to such a calculation can be implicitly written independently of the angle of observation as

$$\delta Q=\tfrac{1}{2}[(E_1^2/M_1c^2)-(E_2^2/M_2c^2)-(E_3^2/M_3c^2)]. \tag{A23}$$

In the case of the techniques used in the experiments reported here, where an electrostatic analyzer was used to measure E_1 and a magnetic analyzer was used to measure E_2, one finds

$$\delta Q\approx-\tfrac{1}{2}[(E_1^2/M_1c^2)+(E_2^2/M_2c^2)+(E_3^2/M_3c^2)]. \tag{A24}$$

This equation holds strictly only for $M_3E_3=M_2E_2$, which will be approximately true for $Q>E_1$. For 90° observation the expression is exact if E_1^2/M_3c^2 is added to the right-hand side.

The Rest Masses

The question arises concerning the correct rest mass to use in Eqs. (A8′) or (A8″)—nuclear or atomic—in transforming Eq. (A6) into Eq. (A9). That the nuclear rather than the atomic mass for the target nucleus should be used seems reasonable from the fact that a nuclear collision happens in a time short compared with characteristic atomic times. A calculation by Christy[47a] indicates that the nuclear mass is indeed the one to use in the usual case in which the excitation energy, which can be imparted to the atom, is so small as to be unresolvable by the spectrometer employed and in which the excitation of the atom to various electronic states results in only small changes in momenta. The tabulated atomic masses are, of course, convenient to use, and for light nuclei,

$$\delta M/M=(M_{\text{nuclear}}-M_{\text{atomic}})/M_{\text{nuclear}}=-Z/1800\text{A}. \tag{A25}$$

Thus, in the experiments reported here we have

$$\delta Q=1/1800[(Z_1E_1/A_3)-(Z_1\mathcal{E}\cos\theta/A_1)-(Z_2E_2/A_2)-(Z_3E_3/A_3)]. \tag{A26}$$

For $Z/A\sim 1/2$ and $Q\approx E_2+E_3>E_1$ we have

$$\delta Q\sim Q/3600, \tag{A26′}$$

which is a negligible correction in all but a few special cases. On the other hand, the use of integral rather than exact atomic weights introduces mass errors of the order of $\delta M/M\sim 0.001$ and hence

$$\delta Q\sim Q/1000. \tag{A27}$$

This error is comparable to the precision obtainable is present Q-measurements and thus the use of integral atomic weights is not advisable. As long as non-integral numbers are to be used,

[47] R. H. Bacon, Am. J. Phys. 8, 154, 354 (1940).

[47a] We are indebted to Professor Christy for communicating his conclusions to us.

we find it just as convenient to use nuclear masses with relativistic corrections as it is to use the tabulated atomic masses.

Energy of Nuclei in Ions

In some instances ions other than the stripped nucleus are used as bombarding agents or are measured as the reaction product. In either case, the fraction of the energy attributable to the nucleus can be calculated on the simple basis of proportionality to rest mass. For example, if HH^+ ions are used in bombardment, each proton has 0.49986 of the total energy of the ion. In the case of capture and loss of electrons in the target we assume that any energy transfers are covered by the empirical or theoretical estimates of the over-all energy losses in the target and contamination layers.

APPENDIX B. ANALYSIS OF ENERGY RELATIONS IN THE TARGET PROCESSES

The use of high resolution devices in the determination of the energy of the incident and emitted particles in a nuclear reaction necessitates a detailed analysis of the reaction events in the target. Figure 17 illustrates the general situation in experiments, such as described in this report, in which the Q-value or the cross section of a nuclear reaction is determined. In practically every calculation involved in such determinations one needs to know the relations between the bombarding energy, E_{1B}, the observed energy of the emitted particles, E_{20}, the average energy, E_1, of the incident particles which actually produce the observed particles, and the energy, E_2, of the emitted particles at production.

In Q-value measurements these relations must be understood in actually determining from the observations the energy, E_{2B}, of the emitted particles produced at the surface of the target by the bombarding particles with their full energy. Neglecting contamination layers to be discussed later, E_{1B} and E_{2B} or E_1 and E_2 but not E_{1B} and E_{20} are the energies which must be substituted into (A11) to yield Q. In cross-section measurements the cross section determined is that for the incident particles with energy E_1. Thus the measurements involve not only the usual counting procedures but also the calculation of E_1 from E_{1B} and E_{20}.

It is clear that these relations will depend primarily on the energy loss of the incident and emitted particles in the target material and secondarily on the scattering and straggling which they undergo. We give here a very elementary discussion in which energy loss considerations are emphasized.

Energy Loss Considerations

For observation of the emitted particles on the same side of the target on which the incident particles impinge, as illustrated in Fig. 17, we have

$$\Delta E_2/\Delta E_1=(E_2-E_{20})(E_{1B}-E_1)=\epsilon_2\cos\theta_1/\epsilon_1\cos\theta_2\equiv\eta, \quad \text{(B1)}$$

where θ_1 and θ_2 are the angles with the normal to the target drawn on the side of the incident beam, and ϵ_1 and ϵ_2 are the stopping cross sections[48] in the target for the incident and emitted particles, respectively. We define η in Eq. (B1) for brevity in what follows. We also have in first approximation

$$E_{2B}-E_2=(\partial E_2/\partial E_1)(E_{1B}-E_1), \quad \text{(B2)}$$

[48] Throughout the calculations using the methods described here we have used stopping cross sections computed from data given by H. A. Bethe, BNLT-7 (1949) (unpublished); C. B. Madsen and P. Venkateswarlu, Phys. Rev. **74**, 648 (1948); C. M. Crenshaw, Phys. Rev. **62**, 54 (1942); R. Wilson, Phys. Rev. **60**, 749 (1941); S. D. Warshaw, Phys. Rev. **76**, 1759 (1949). We have used interpolation methods for elements for which measurements have not been made. This is satisfactory in the evaluation of small correction terms in energy measurements but does constitute a source of error of ~10 percent in cross-section measurements. Following the practice of M. S. Livingston and H. A. Bethe, Revs. Modern Phys. **9**, 270 (1937), we have used ϵ in units of 10^{-15} ev cm^2.

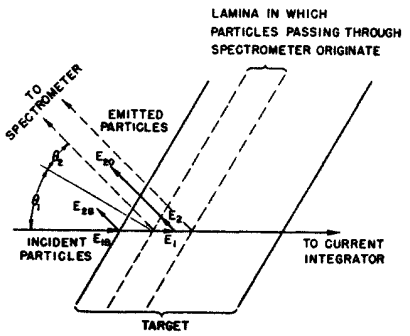

FIG. 17. Analysis of energy relations in the target processes taking into account only energy loss effects and neglecting scattering and straggling.

where $\partial E_2/\partial E_1$, is given by Eq. (A20). From these two equations we obtain:

$$\frac{\Delta E_1}{\Delta E_{20}}=\frac{E_{1B}-E_1}{E_{2B}-E_{20}}=\frac{\epsilon_1}{\epsilon_{\text{eff}}}=\left(\eta+\frac{\partial E_2}{\partial E_1}\right)^{-1} \quad \text{(B3)}$$

$$\frac{\Delta E_2}{\Delta E_{20}}=\frac{E_2-E_{20}}{E_{2B}-E_{20}}=\frac{\epsilon_2\cos\theta_1}{\epsilon_{\text{eff}}\cos\theta_2}=\left(1+\frac{1}{\eta}\frac{\partial E_2}{\partial E_1}\right)^{-1}. \quad \text{(B4)}$$

In these equations we have defined an effective over-all stopping cross section as

$$\epsilon_{\text{eff}}=\epsilon_1(\partial E_2/\partial E_1)+\epsilon_2\cos\theta_1/\cos\theta_2. \quad \text{(B5)}$$

These equations reflect in the spread of the energy of the observed particles, ΔE_{20} not only their loss of energy, ΔE_2, in the target, but also the variation in their energies at production arising from the loss of energy, ΔE_1, of the incident particles in the target. We place ΔE_{20} in the denominator of (B3) and (B4), as it will be the observable from which ΔE_1 and ΔE_2 can be calculated. A similar derivation for the case of the particles being observed after transmission through the target leads to the same result if θ_2 is measured as before and if E_{2B} is the observed energy of those particles produced at the front surface of the target *after* their passage through the target with consequent energy loss. Our results (B3) and (B4) thus hold in general.

Equations (B3) and (B4) are useful in determining E_1 and E_2 if E_{1B}, E_{2B}, and E_{20} are measured. At this point we wish to discuss the determination of E_{2B}. In the case illustrated we note that $\cos\theta_1$ and $\cos\theta_2$ are both positive. Then since $\partial E_2/\partial E_1$ is usually positive, E_{2B} will be the maximum energy observed for the emitted particles and, aside from some complications arising from the finite resolution of the spectrometer, it can be readily measured experimentally. In fact, in either method of observation E_{2B} will be the maximum E_{20} for $\epsilon_{\text{eff}}>0$. However, in the transmission case the absolute energy losses must be ascertained to complete the Q-value calculations. In case $\epsilon_{\text{eff}}<0$, then E_{2B} will be the minimum E_{20}, while for $\epsilon_{\text{eff}}=0$, all the observed particles will have the same energy. These last two cases may arise in transmission observations when $\cos\theta_2<0$ or in observations at certain angles on residual nuclei when $\partial E_2/\partial E_1<0$. In these cases, however, straggling in energy plays an important role. In the case $\epsilon_{\text{eff}}=0$, straggling will determine completely the spread in energy of the emitted particles, while for $\epsilon_{\text{eff}}<0$, straggling will make it difficult to choose E_{2B} from the observations, especially in the transmission case. It might be argued that the maximum observed energy should always be employed with appropriate treatment in the calculations. However, for $\epsilon_{\text{eff}}<0$, the maximum energy particles observed will be those produced at the back side of the target, and their energy will depend on energy losses in the target. Straggling in this loss and errors in its measurement will contribute considerable uncertainty to such a determination.

For the reasons just discussed, in the experiments reported in this paper, observations have been made on the side of the target on which the incident particles impinge and on the lighter of the

two reaction products, so that $\epsilon_{eff}>0$. In this way it has been possible to use thick targets for mechanical and other reasons and to use the spectrometer resolution to isolate reaction products from determinable lamina in these targets. A case in which $\partial E_2/\partial E_1<0$ and $\epsilon_{eff}\approx 0$ has been discussed previously.[49] It must also be noted that for $\epsilon_{eff}\approx 0$, variations in ϵ_1 and ϵ_2 with energy will also make contributions to the spread in energy of the observed particles, it being possible for particles of a given observed energy to originate in two separate lamina in the target if, for example, ϵ_{eff} varies from a small positive value through zero to a small negative one over the range of particle energies involved in the target events.

Equation (B3) can be solved for E_1 to yield

$$E_1=\frac{\eta E_{1B}+E_{20}+[E_{1B}(\partial E_2/\partial E_1)-E_{2B}]}{\eta+(\partial E_2/\partial E_1)}, \qquad (B3')$$

where the term in brackets is zero in the case of elastic scattering and in any case is a constant for a given reaction over any small range of energies. The independent variables in the experiments are E_{1B} and E_{20} and convenient relations in certain calculations are

$$\partial E_1/\partial E_{1B}=(1+\eta^{-1}\partial E_2/\partial E_1)^{-1} \qquad (B6)$$

$$\partial E_1/\partial E_{20}=(\eta+\partial E_2/\partial E_1)^{-1}. \qquad (B7)$$

These partial derivatives make it possible to determine numerically any interval or fluctuation in E_1 in terms of the corresponding intervals or fluctuations in E_{1B} and E_{20}. This will be important, for example, in determining the energy resolution or errors in cross section *vs* energy measurements (excitation curves).

The Effective Target Thickness in Thick Target Measurements

The application of the above energy loss arguments to any thin lamina in the target leads to relations similar to (B3) and (B4). For example, if δE_{20} represents the energy interval over which the spectrometer accepts particles because of its finite exit window, then the energy loss of the incident particles in the lamina from which the observed particles are emitted is

$$\xi_1=\epsilon_1 nt=\frac{\epsilon_1\delta E_{20}}{|\epsilon_{eff}|}=\frac{\delta E_{20}}{|\eta+\partial E_2/\partial E_1|}=\frac{2E_{20}}{R_c|\eta+\partial E_2/\partial E_1|}, \qquad (B8)$$

where R_c is the resolution (in momentum) calculated, taking into account only the exit (or collector) slit width. It is given by

$$R_c=2(1+M)r_0/\delta r_c, \qquad (B8')$$

where M is the magnification of the instrument (0.8 in these experiments), δr_c is the collector slit width, and r_0 is the radius of curvature of the particle orbit. As long as the actual target is thicker than ξ_1, other sources of finite resolution do not enter into the probability of detection and in any case integrals over the thin target distribution depend only on R_c. Expression (B8) is useful for determining nt in cross-section measurements where n is the number of nuclei per cubic centimeter of target and t is the effective target thickness parallel to the incident beam. Again considerable caution must be observed when $|\epsilon_{eff}|\approx 0$ since then, straggling and variations in ϵ_1 and ϵ_2 with energy play dominant roles in determining the effective target thickness.

Corrections for Contamination Surface Layers

In the body of this report we have reported our finding of thin layers of carbon and oxygen on certain types of targets even with liquid air traps and diffusion pumps connected directly to the target chambers. We have emphasized that the use of the magnetic spectrometer in the detection of reaction and scattering products has made it possible to ascertain the thickness of these layers throughout the observations and to make appropriate corrections for them. We here wish to discuss the magnitude of these corrections.

The thickness of the layers is usually most directly expressed in terms of the energy loss of the incident particles in them. This is because observations on the amount of scattering by the layers and on the change in energy of the particles scattered by the true target under the layers can be accomplished so conveniently with the spectrometer. In the experiments described in this report we have used protons as incident particles and have found the energy loss in the layers in one traversal normal to the target to be, in general, of the order of 0.5 kev for 1-Mev protons. As the layers are about equally carbon and oxygen, it is sufficiently accurate to use the readily available stopping cross sections for air in calculations of the thickness. For 1-Mev protons the value is 5×10^{-15} ev-cm^2, so $nl\approx10^{17}$ atoms/cm^2 where l is the thickness of the layer. Using a density of one, it is found that these layers are the order of 100 atoms thick or $l\approx3\times10^{-6}$ cm.

The correction for surface layers to be applied to Q, if the bombarding incident energy and the observed product energy are used in the preliminary calculations, is

$$\delta Q=\frac{\epsilon_2 nl}{\cos\theta_2}\frac{\partial Q}{\partial E_2}-\frac{\epsilon_1 nl}{\cos\theta_1}\frac{\partial Q}{\partial E_1}$$

$$\approx 0.1\left(\frac{\epsilon_2}{\cos\theta_2}\frac{\partial Q}{\partial E_2}-\frac{\epsilon_1}{\cos\theta_1}\frac{\partial Q}{\partial E_1}\right)\text{ kev}$$

$$\approx 0.1\left(\frac{\epsilon_2}{\cos\theta_2}\frac{M_2+M_3}{M_3}+\frac{\epsilon_1}{\cos\theta_1}\frac{M_3-M_1}{M_3}\right)\text{ kev at }90°. \qquad (B9)$$

In the approximate expressions the ϵ are in the usual units employed, namely 10^{-15} ev cm^2 or 10^{-18} kev cm^2. The partial derivatives can be obtained from (A14, 15). As an example, the correction for $B^{10}(p,\alpha)Be^7$, where $\theta=138°$, $\theta_1=28°$, $\theta_2=14°$, and $E_1\sim E_2\sim 1$ Mev is

$$\delta Q\approx 0.1[(46\times1.77/0.97)+(5\times0.66/0.88)]\approx 8.8\text{ kev}. \qquad (B9')$$

Because of the large value of this correction, E_1 and E_2 were carefully corrected before substitution in the Q-equation for layers measured before and after the direct observations. Also, in determining the excitation energy of Be^{7*}, the incident proton energy was adjusted so that the two alpha-particle groups had about the same energy and thus their large losses approximately cancelled in calculating the excitation energy.

The Effects of Straggling

In the previous discussion we have emphasized that the straggling in the energy loss of the incident and outgoing particles introduces considerable uncertainty in the results of transmission experiments and even in the reflection experiments when $\partial E_2/\partial E_1$ is negative enough to make $\epsilon_{eff}<0$. Fortunately, in the experiments here discussed $dE_2/dE_1>0$, and we have observed at angles for which the reflection method is convenient. Here, we wish to discuss straggling effects in somewhat more detail for this case.

The mean square deviation in energy loss is given with sufficient accuracy for our purposes by the early formula of Bohr:

$$\langle(dE-\Delta E)^2\rangle=4\pi e^4z^2Znt$$
$$=260z^2Z\Delta E/\epsilon\text{ (ev)}^2, \qquad (B10)$$

where ze is the charge of the incident particle, Z is the atomic number of the target material, $\Delta E=\langle dE\rangle$ is the mean energy loss in ev, and ϵ is the stopping cross section in units 10^{-15} ev cm. In measurements on the straggling of 1 Mev protons in Be we find this expression gives a value for the root-mean-square deviation low by only 30 percent and, since this is an extreme case, (B10) is accurate enough for use in small correction terms. Using the customary approximate expression[40] for ϵ we have

$$\langle(dE-\Delta E)^2\rangle=E\Delta E[2m_0/M\ \ln(4m_0E/M\bar{I})], \qquad (B11)$$

or

$$[\langle(dE-\Delta E)^2\rangle]^{\frac{1}{2}}=1/30(E\Delta E/M)^{\frac{1}{2}}(\ln E/5200MZ)^{-\frac{1}{2}}. \qquad (B12)$$

[49] Tollestrup, Jenkins, Fowler, and Lauritsen, Phys. Rev. **75**, 1947 (1949).

In (B12) the mass of the particle M is in atomic mass units and the average ionization potential, $\bar{I}$, of the stopping material has been evaluated as $11.5Z$ ev. In the logarithm term, E must be in ev. In the region of usual interest ($E\sim 1$ Mev for protons) the slowly varying logarithmic term ~ 3 and

$$[\langle(dE-\Delta E)^2\rangle]^{\frac{1}{2}}\sim 0.02(E\Delta E/M)^{\frac{1}{2}}. \tag{B13}$$

The straggling will be in the same units as E and the energy loss ΔE. In our estimates of the straggling effects we add, linearly, the mean square deviations in energy loss for the incident and outgoing particles, using coefficients determined in the section on energy relations in the target.

In the reflection experiments, when $\epsilon_{\text{eff}}>0$, there is little effect of straggling on the energy of the particles produced at the front surface of the target. The ideal step function is of course rounded off slightly but this rounding off occurs completely in an energy interval which is at most of the order of the maximum energy transfer in a single collision to atomic electrons by the particles involved. This transfer is just $4m_0/M$ times the energy of the particle and even for protons is only ~ 0.002 of the proton's energy. This is well obscured by other sources of finite resolution in the experiments here described, and, in any case, the effect on the average behavior of the particles at the surface can be expected to be smaller. As a consequence, straggling can be neglected in the determination of E_{2B} except in so far as contamination layers are important.

In a surface contamination layer in which the apparent shift in the observed energy of the outgoing particles is

$$\Delta E_{20}=(\partial E_2/\partial E_1)\Delta E_1+\Delta E_2, \tag{B14}$$

the straggling will be given by summing the squares of the contribution of the incident and outgoing particles, *viz.*:

$$\delta E_{20}^2=[(\partial E_2/\partial E_1)\delta E_1]^2+\delta E_2^2, \tag{B15}$$

where δE_1 and δE_2 can be any arbitrary measures of the straggling. They will always be proportional to the root mean square deviation in energy loss given by (B10 to 13). Neglecting other sources of finite resolution the rise at the high energy end of the observed energy distribution will be given by the integral of the error function and a tangent line drawn through the midpoint will rise to the full value in $(2\pi)^{\frac{1}{2}}\sim 2.5$ times the root mean square deviation. Using this as a measure of the straggling we have

$$\begin{aligned}\delta E_{20}^2&=1600Z[(z_1\partial E_2/\partial E_1)^2(\Delta E_1/\epsilon_1)+z_2^2(\Delta E_2/\epsilon_2)](\text{ev})^2\\&=1600Z(\Delta E_{20}/\epsilon_{\text{eff}})[(z_1\partial E_2/\partial E_1)^2+z_2^2\cos\theta_1/\cos\theta_2](\text{ev})^2\end{aligned} \tag{B16}$$

for ϵ_{eff} in 10^{-15} ev-cm^2. We note that

$$\Delta E_{20}/\epsilon_{\text{eff}}=\Delta E_1/\epsilon_1=nl/\cos\theta_1\times 10^{-15}$$

$nl\approx 10^{17}$ cm^{-2} for the observed layers, and $Z=7.22$ if we use ϵ for air. Hence,

$$\delta E_{20}=1.1[(z_1\partial E_2/\partial E_1)^2/\cos\theta_1+z_2^2/\cos\theta_2]^{\frac{1}{2}}\ \text{kev}_1. \tag{B17}$$

For the $B^{10}(p,\alpha)Be^7$ example of the preceding section we have $\Delta E_{20}=4.9$ kev and $\delta E_{20}=3.2$ kev. Since $\delta E_{20}<\Delta E_{20}$, this small straggling effect is a symmetrical one, and the method of determination of E_{2B} is not effected.

The straggling in the target itself has its major effect on the low energy side of the distribution of observed particles. If ΔE_{20} is the average apparent energy loss in the target then Eq. (B16) gives the interval δE_{20} over which the tangent to the midpoint of the low energy side falls from the maximum reading to zero. As long as $\delta E_{20}<\Delta E_{20}$, as is the case for even the thinnest targets we have used, the straggling is symmetrical about the mean loss, and the distribution in energy of the observed particles has a flat maximum extending over the interval $\sim\Delta E_{20}-\frac{1}{2}\delta E_{20}$ followed by a drop to zero over the interval $\sim\delta E_{20}$. This is illustrated in Fig. 7 of reference 15 which shows the scattering of protons by a Be foil using very high resolution in the spectrometer. It can be shown that the maximum number of processes detected is just that to be expected in the ideal case neglecting straggling, and thus in calculating reaction cross sections it is justifiable to use the stopping cross sections, which are based on average energy losses, in Eq. (5) of the main body of this report. The straggling in the target is also a source of finite resolution in energy determinations in excitation curve measurements. The effects of straggling in this connection will be discussed in a forthcoming paper on scattering measurements.

Determination of E_{2B} in Thin Target Measurements

When thin targets are employed in Q-determinations the position in the observed energy distribution of the particles produced at the target surface depends on the effective target thickness for the emitted particles and the over-all resolution of the spectrometer. It is clear that E_{2B} is given by the average energy of the observed particles plus one-half the effective target thickness for those particles in energy units. This effective thickness will just be the energy loss of the incident particles in the target multiplied by $\partial E_2/\partial E_1$ plus the energy loss of the emitted particles in traversing the target. It is most directly obtained by weighing the target and determining its area and then using the empirical values of the stopping cross sections and the angles of traversal. This is not always feasible, however, and measurements on the energy distribution of the incident particles scattered by the target can be employed readily to yield its thickness for a given energy of the incident particle. Only the variation of the stopping cross section with energy and not the absolute values need be used in such a calculation. Similarly, to obtain the energy loss of the emitted particles and the effective thickness for them, it is only necessary to know the ratio of the stopping cross sections ϵ_2/ϵ_1. When it is possible to do so, the effective thickness is most easily determined by comparing the integrated yield for the target with the maximum yield for a thick target of the same material. From Eqs. (5) and (9) of the text one has directly

$$\xi_{\text{eff}}=\frac{E_{20}}{N_{\max}}\int\frac{NdE}{E}=\frac{2E_{20}}{N_{\max}}\int\frac{NdI}{I}, \tag{B18}$$

where $N_{\max}$ represents the maximum number of counts obtainable with a thick target and is the N appearing in Eq. (5′).

The determination of the average energy of the observed particles involves the use of particles which have suffered large losses, and it is sometimes preferable to estimate the instrumental spread[50] in the energy of the observed particles and to use the ratio of ξ_{eff} to δE_{20} to predict the relative number of counts at E_{2B}. As an illustration we consider the instrumental spread to be gaussian, and in keeping with our practice we take $(2\pi)^{\frac{1}{2}}$ times the root-mean-square deviation as δE_{20}. We let the effective energy loss be spread uniformly over ξ_{eff} without straggling. Then if $T=(2\pi)^{\frac{1}{2}}\xi_{\text{eff}}/\delta E_{20}$, we have

$$\frac{N(I_B)}{N_{\max}}=\frac{1}{2}\left(\int_{-T}^{T}\exp(-t^2/2)dt\right)\Big/\left(\int_{-T/2}^{T/2}\exp(-t^2/2)dt\right), \tag{B19}$$

where I_B is the fluxmeter reading from which E_{2B} is calculated. For $\xi_{\text{eff}}\gg\delta E_{20}$, this approaches $\frac{1}{2}$, as expected for a thick target, while for $\xi_{\text{eff}}\ll\delta E_{20}$, it approaches unity, as expected for a very thin target. For $\xi_{\text{eff}}=\delta E_{20}$, $N(I_B)/N_{\max}=0.63$ and for $\xi_{\text{eff}}=\delta E_{2B}/2$, $N(I_B)/N_{\max}=0.84$. The determination of the point at which $N(I_B)/N_{\max}$ has its calculated value can often be done with considerable precision on the front side of the observed curve, and E_{2B} is thus given accurately.

The Determination of E_{2B} in Thick Target Measurements

We have found that the most precise determinations are yielded by thick target curves. In this case, to the approximation discussed above, $N(I_B)/N_{\max}=\frac{1}{2}$, but in some cases it is worthwhile to consider additional effects. These are the effects of the

[50] We use δE_{20} for the instrumental spread in E_{20} in this section while we used it for the straggling in E_{20} in the preceding section.

dependence of the cross section of the process, the stopping cross sections, and the probability of detection of the emitted particle on energy. For no instrumental spreads other than that arising from the width of the exit slit, the number of counts at the fluxmeter reading I_0 corresponding to the energy, E_{20}, is proportional to the following energy dependent terms:

$$N(I_0)\sim nt\sigma(E_1)\sim E_{20}\sigma(E_1)/\epsilon_{\text{eff}}(E_1,E_2), \tag{B20}$$

where σ must be evaluated at E_1, the energy of the incident particles at which the reaction actually occurs (Fig. 17) and ϵ_{eff} must be evaluated at appropriate average energies in the intervals E_{1B} to E_1 and E_2 to E_{20}. As an illustration we consider the behavior of this function in the case of Rutherford elastic scattering for which $\sigma\sim E_1^{-2}$. If we assume the scattering nuclei are heavy compared to the incident particles, we have $\partial E_2/\partial E_1=1$ and $E_1=E_2=\frac{1}{2}(E_{2B}+E_{20})$. The stopping cross section can be taken as inversely proportional to the square root of the energy (Geiger's law) and hence

$$N\sim E_{20}\Big/\left(\frac{E_{2B}+E_{20}}{2}\right)^{\frac{1}{2}}. \tag{B21}$$

For E_{20} not too far below E_{2B}, this becomes

$$N\sim E_{20}^{\frac{1}{2}}/E_{2B}^{\frac{1}{2}}\sim I_B^{\frac{1}{2}}/I_0^{\frac{1}{2}}\to I_B \quad \text{for} \quad I_0=I_B. \tag{B22}$$

The observed number drops away slowly from a maximum number which is proportional to $E_{2B}^{-\frac{1}{2}}=E_{1B}^{-\frac{1}{2}}$ or to I_B. We have verified this experimentally in considerable detail in the scattering of protons by copper.

Returning to the general expression (B20) we now consider the effect of the instrumental spread in energy which, for convenience in calculation, we now assume to be rectangular in distribution with width $\delta E_{20}=2E_{20}/R$ in energy or with width $\delta I=I/R$ on the fluxmeter scale. In the energy range of interest we approximate the yield by

$$N\sim E_{20}{}^{n/2}\sim I_0{}^{-n},$$

where by comparison with (B20) we have

$$n=2+a+(2d\sigma/\sigma dE_1)(\epsilon_1 E_{2B}/\epsilon_{\text{eff}}).$$

In this expression the member a is a complicated term arising from the dependence of (B20) on ϵ_{eff} and is given by

$$\begin{aligned} a&=0, \quad \epsilon_2\cos\theta_1/\cos\theta_2\gg\epsilon_1\partial E_2/\partial E_1\\ a&\sim\tfrac{1}{2}, \quad \epsilon_2\cos\theta_1/\cos\theta_2\sim\epsilon_1\partial E_2/\partial E_1\\ a&=1, \quad \epsilon_2\cos\theta_1/\cos\theta_2\ll\epsilon_1\partial E_2/\partial E_1. \end{aligned}$$

To determine n, the relation σ *vs* E_1 must be known or must be measured, independently. Then the effect of the finite resolution yields

$$N(I_B)/N_{\max}=\tfrac{1}{2}(1+n/4R).$$

Alternatively, I_B from which E_{2B} is calculated can be found by adding $n\delta I_B/8=nI_B/8R$ to the reading at half-maximum. Whaling and Li have found this correction to be appreciable in the $Li^7(p,\alpha)He^4$ reaction.[51]

APPENDIX C. ERRORS OF THE MEASUREMENTS

Sources which contribute to errors in measurements of E_1, E_2, and θ and hence of Q have been enumerated previously.[15] As is customary, they can be classified as either systematic or statistical errors. It has been our experience in performing measurements with the electrostatic analyzer and magnetic spectrometer discussed in this paper that the statistical errors in a Q-value, determined under widely differing conditions (different bombarding energies, targets, and angles of observation) over long periods of time, could be reduced to very small values compared to realistic estimates of the systematic errors. Fluctuations in the incident beam energy, in the measurement of the fluxmeter reading, in the relative values of the field over the particle path, in the target, collector, and stop positions have apparently contributed statistical probable errors of 0.1 percent.

[51] W. Whaling and C. W. Li, Phys. Rev. **81**, 150 (1951).

We have not attempted to make absolute energy measurements but have depended on the standard nuclear energy scale established through the careful work of Herb and his collaborators at the University of Wisconsin.[42b] One systematic error is as follows: (1) the published probable error in the energy of the resonance used directly in the calibration of the electrostatic analyzer and indirectly in the calibration of the magnetic spectrometer. Others are, (2) the nonlinearity of the scales of the analyzer and spectrometer, (3) the uncertainty in the interpretation of the line shape of the observed particles as reflected in the choice of E_{2B}, (4) errors in the estimate of surface layer corrections arising from uncertainty in the scattering and stopping cross sections and, (5) the error in measurement of the angle of observation.

If the errors in E_1, E_2, and θ are completely independent, then the error in Q can be calculated from

$$\delta Q^2=\left(\frac{\partial Q}{\partial E_1}\delta E_1\right)^2+\left(\frac{\partial Q}{\partial E_2}\delta E_2\right)^2+\left(\frac{\partial Q}{\partial\theta}\delta\theta\right)^2 \tag{C1}$$

with the partial derivatives being found in Eqs. (A13 to 15). In our method of calibration of the spectrometer, however, part of the error in E_2 is dependent on the errors in E_1 and θ. By the use in these calibrations of scattering materials such as Cu, for which $M_0\gg M_1$, we made the contribution of any error in θ to the error in E_2 practically negligible. We also used high energy particles so that layer errors were minimized. On the other hand, the relative error in E_2 is equivalent to that in E_1 of the calibrating particles, since $\partial E_2/\partial E_1=E_2/E_1$ in scattering processes [see (A12) and (A20) for $Q=0$]. It is then easy to show that $(\partial Q/\partial E_1)$ in (C1) must be replaced by Q/E_1, and δE_2 must be taken as just the independent errors in E_2. Since Herb gives the probable error of his determinations of the $F^{19}(p,\alpha'\gamma)$ and $Al(p,\gamma)$ resonances as 0.1 percent, a contribution to the first term in (C1) is $(0.001Q)^2$.

Another interdependent error in E_1 and E_2 is number (4) above, the surface layer error. The correction we make for surface layers can be in error by $\delta\xi/\xi\sim 20$ percent just because scattering and stopping cross sections are uncertain to about this amount. The error is thus about 0.1 kev for 1-Mev protons or 0.01 percent. The contribution to the error in Q is $(-\partial Q/\partial E_1+\eta\partial Q/\partial E_2)\delta\xi_1\sim(1+\eta)E_1\times 10^{-4}$. Note that the terms in the coefficient of $\delta\xi_1$ are usually of the same sign, since $\delta E_1=-\delta\xi_1$ and $\delta E_2=\eta\delta\xi_1$.

Careful measurements with H^+, HH^+, and HHH^+ ions, as described previously,[15] have not revealed any indication of a systematic nonlinearity in the scales of the analyzer and spectrometer. One possible source of nonlinearity—the stray field of the magnetic spectrometer—has been shown by Mr. William Warters of this laboratory to be closely proportional to the field in the magnetic gap over the full range of fields used in these experiments. We have, in addition, attempted to perform calibration experiments at the same energies as in the direct measurements.

The determination of E_{2B} from the observed distribution in E_{20} has been discussed in Appendix B. In clean-cut cases in which the cross sections are known, the backgrounds are small, and the surface layer effects are small, the location of E_{2B} involves only negligible error. This is the case for $Li(p,p)Li^7$ and $B^{10}(p,\alpha)Be^7$. In the cases $Li^7(p,p')Li^{7*}$ and $B^{10}(p,\alpha')Li^{7*}$, the background and layers were especially troublesome, and we estimate the systematic independent probable error from this cause to be $0.001E_2$ in the first case and $0.0015E_2$ in the second case. Multiplication by $\partial Q/\partial E_2$ yields the contribution to the error in Q.

The error in Q arising from the error in the measurement of the angle of observation can be relatively large. For E_1 and E_2 in Mev we have from (A10) and (A13)

$$\partial Q/\partial\theta=35(M_1M_2E_1E_2/M_3^2)^{\frac{1}{2}}\sin\theta \text{ kev/degree}. \tag{C2}$$

The corrections can be minimized by observations near 0° or 180° but this is often not practical for other reasons. In these experiments we have been primarily interested in the excitation energies of Li^{7*} and Be^{7*}. By measurements of the Q's involving the ground and excited states without changing the position of the spectrom-

eter and thus without changing θ, we have been able to minimize the effect of the systematic error in θ. We actually compute $E_x=\Delta Q=Q-Q^*$ from

$$\Delta Q=\frac{M_3+M_2}{M_3}(E_2-E_2')-\frac{M_3-M_1}{M_3}(E_1-E_1')$$
$$-2\cos\theta\frac{(M_1M_2)^{\frac{1}{2}}}{M_3}[(E_1E_2)^{\frac{1}{2}}-(E_1'E_2')^{\frac{1}{2}}], \quad (C3)$$

where the unprimed quantities are determined in $Li^7(p,p)Li^7$ or $B^{10}(p,\alpha)Be^7$ and the primed ones in $Li^7(p,p')Li^{7*}$ or $B^{10}(p,\alpha')Be^{7*}$. It is clear that the systematic error in θ can even be reduced to zero by appropriate choices (not independent) of the E's such that $(E_1E_2)^{\frac{1}{2}}-(E_1'E_2')^{\frac{1}{2}}=0$. Also, it can be shown that if the scales for E_1 and E_2 are calibrated against the same primary standard, $\delta\Delta Q=(\Delta Q/E_1)\delta E_1=(\Delta Q/E_2)\delta E_2$. In the Be^{7*} case, we choose $E_2'\sim E_2$ in order to minimize the large errors arising from uncertainty in the energy losses of the outgoing alpha-particles. This also reduced the error from θ to 30 percent of its effect on the main Q-value. In the Li^{7*} case, for intensity reasons, we choose $E_1=E_1'$. It should be emphasized that the systematic error in the location of E_{2B} is large only in determining Q^* and so this error is not reduced in the calculation of ΔQ. The various errors and the final values are discussed and tabulated in the text (Tables III and V).

PHYSICAL REVIEW VOLUME 82, NUMBER 2 APRIL 15, 1951

Spin-Orbit Coupling in Li^7 and Be^7

D. R. INGLIS
Argonne National Laboratory, Chicago, Illinois
(Received January 2, 1951)

The magnetic spin-orbit coupling of the p-shell nucleons is shown to have the correct sign and about half the magnitude to account for the 45-kev difference of the first excitation energies, 479 kev in Li^7 and 434 kev in Be^7, if these are interpreted as doublet splittings arising mainly from a spin-orbit coupling term of the same form as the Thomas term but stronger and presumably of mesonic origin, such as seems to be responsible for the appearance of (jj) coupling in heavy nuclei. Be^7 is expected to be slightly larger than Li^7 because of the added coulomb repulsion, so that the average value of the main term is expected to be smaller for Be^7, and it is estimated that this coulomb expansion explains another one-fourth to the splitting difference, leaving about one-forth unaccounted for. These estimates are made both very simply by means of the droplet model and more reliably by minimizing the energy obtained with exchange interactions and three-dimensional isotropic oscillator wave functions. Energies attributed to spin-orbit coupling in other nuclei indicate that the main term should make the Li^7 and Be^7 doublet splittings about 50 percent larger than observed. This suggests that second-order perturbations may reduce both by nearly the same amount, leaving their estimated difference significant. The possibility of more drastic perturbations and their relation to the quadrupole-moment problem are discussed. The agreement of the estimated splitting difference in sign and order of magnitude is consistent with other evidence favoring the (LS)-coupling interpretation that the two low states form a ^2P.

I. INTRODUCTION

ONE very interesting feature of the 434-kev state in Be^7 is that its excitation energy is approximately[1] but not exactly equal to that of the 479-kev state in the mirror nucleus Li^7. One, of course, assumes that they are mirror states,[2] or that they differ only in isotopic spin and coulomb energy, and the current experimental situation[3] favors the conclusion that they have nuclear spin $I=\frac{1}{2}$ in spite of the intensity-ratio difficulty in the thermal reaction $B^{10}(n,\alpha)Li^{7*}$, Li^7. This permits one to assume[4] that this state, together with the ground state, forms a ^2P. The magnitude of the 479-kev doublet splitting has long presented a problem of interpretation in terms of nuclear spin-orbit coupling, and now the 45-kev difference between the two doublet splittings enriches the opportunity for testing simultaneously the interactions responsible for spin-orbit coupling, the theory of nuclear structure, and the ^2P assignment. The original interpretation[4] of this splitting was given in terms of the picture of a nucleus consisting of nucleons as its fundamental constituents, with their binding forces treated phenomenologically, and with no attention paid to the source of these forces. The relativistic kinematic effect known as the Thomas precession was seen as the primary source of the splitting, modified by the magnetic effect. This simple theory automatically gives the correct sign of spin-orbit coupling to account for the nuclear spins of the ground states of most fairly simple nuclei (whereas subsequent theories of spin-orbit coupling unfortunately leave an arbitrary choice of sign). For this reason it remained attractive even after it became increasingly apparent that it was inadequate to account for the magnitude of the 479-kev splitting in Li^7, because of the possibility that a narrower doublet might be hidden in the rather broad ground-state group of the range measurements, until rather recent magnetic analysis[5] showed the ground state to be single within a few kev. The recent success of the (jj) coupling shell model[6] indicates the presence of strong spin-orbit coupling in heavy nuclei

[1] Brown, Snyder, Fowler, and Lauritsen, Phys. Rev. **82**, 159 (1951).
[2] As is verified by the approximately equal gamma-ray intensities in the mirror reactions.
[3] B. Rose and A. R. W. Wilson, Phys. Rev. **78**, 68 (1950); B. T. Feld, Phys. Rev. **75**, 1618 (1949); S. Devons, Proc. Phys. Soc. (London) **62A**, 580 (1949); D. R. Inglis, Phys. Rev. **81**, 914 (1951).
[4] D. R. Inglis, Phys. Rev. **51**, 783 (1936).
[5] Buechner, Strait, Stergiopoulos, and Sperduto, Phys. Rev. **74**, 1569 (1948).
[6] M. G. Mayer, Phys. Rev. **78**, 16, 22 (1950); D. Kurath, Phys. Rev. **80**, 98 (1950); Haxel, Jensen, and Suess, Naturwiss. **36**, 155 (1949).